

# Vacuum densities and the Casimir forces for branes orthogonal to the AdS boundary

S. Bellucci<sup>1\*</sup>, A. A. Saharian<sup>2†</sup>, V. Kh. Kotanjyan<sup>2,3‡</sup>

<sup>1</sup> *INFN, Laboratori Nazionali di Frascati,  
Via Enrico Fermi 54, 00044 Frascati, Italy*

<sup>2</sup> *Department of Physics, Yerevan State University,  
1 Alex Manoogian Street, 0025 Yerevan, Armenia*

<sup>3</sup> *Institute of Applied Problems of Physics NAS RA,  
25 Hrachya Nersissyan Street, 0014 Yerevan, Armenia*

August 2, 2022

## Abstract

For a massive scalar field with general curvature coupling we evaluate the Wightman function in the geometry of two parallel branes perpendicular to the AdS boundary. On the separate branes, the field operator is constrained by Robin boundary conditions, in general, with different coefficients. In the region between the branes their contribution to the Wightman function is explicitly separated. By using this decomposition, the brane-induced effects on the vacuum expectation values (VEVs) for the field squared and energy-momentum tensor are investigated. The behavior of those expectation values is studied in various asymptotic regions of the parameters. The vacuum energy-momentum tensor in addition to the diagonal components has a nonzero off-diagonal stress. Depending on the boundary conditions and also on the distance from the branes, the vacuum energy density can be either positive or negative. The Casimir forces acting on the branes have two components. The first one corresponds to the standard normal force and the second one is parallel to the branes and presents the vacuum shear force. Unlike to the problem of parallel plates in the Minkowski bulk, the normal Casimir forces acting on separate branes differ if the boundary conditions on the branes are different. They can be either repulsive or attractive. In a similar way, depending on the coefficients in the boundary conditions, the shear force is directed toward or from the AdS boundary. The separate components may also change their signs as functions of the interbrane separation. At large proper separations between the branes, compared to the AdS curvature radius, both the components of the Casimir forces exhibit a power-law decay. For a massive scalar field this behavior is in contrast to that for the Minkowski bulk, where the decrease is exponential.

Keywords: Casimir effect, AdS spacetime, branes

## 1 Introduction

Motivated by fundamental questions and applications in condensed matter physics, cosmology and in high-energy physics, the Casimir effect (for reviews see [1]) remains to be an active field of research

---

\*E-mail: bellucci@lnf.infn.it

†E-mail: saharian@ysu.am

‡E-mail: vatokoto@gmail.com

in quantum field theory. The effect is an interesting manifestation of quantum fluctuations of fields influenced by the presence of boundaries or by nontrivial spatial topology. Depending on the model under consideration the physical nature of the boundaries can be different. Examples are the interfaces of macroscopic bodies in quantum electrodynamics, boundaries separating different phases of the system, horizons in gravitational physics, branes in string theories and in cosmological models of braneworld type, etc. The boundary and periodicity conditions imposed on the operator of a quantum field modify the spectrum of fluctuations and result in the shift of the expectation values of physical quantities such as energy-momentum tensor or current densities for charged fields.

In addition to the boundary or periodicity conditions imposed on the field, the properties of quantum fluctuations are sensitive to the presence of background classical fields. Those fields reduce the symmetry in respective problems and exact results for physical characteristics in the Casimir effect are obtained for highly symmetric bulk and boundary geometries only. In the present paper we consider the influence of the background gravitational field on the properties of the scalar vacuum in the geometry of two parallel branes in background of anti-de Sitter (AdS) spacetime. That geometry is the maximally symmetric solution of the Einstein field equations with a negative cosmological constant as the only source of the gravitational field. As it will be shown below, this high symmetry allows to obtain closed analytic expressions for the expectation values characterizing the local properties of the vacuum state. In addition to the high symmetry, our choice of AdS spacetime as the background geometry is motivated by its important role in two exciting developments of theoretical physics during the last decade, namely, AdS/conformal field theory (CFT) correspondence and braneworld scenarios with large extra dimensions. The AdS/CFT correspondence (for reviews see, e.g., [2]) establishes duality between two different theories: supergravity or string theory on asymptotically AdS bulk from one side and conformal field theory on AdS boundary from another one. Those theories live in different numbers of spacetime dimensions and the correspondence is an example of holographic duality. It provides an important possibility to investigate strong coupling non-perturbative effects in one theory by mapping them to weak coupling region of dual theory and has been applied in different physical settings including the variety of condensed matter systems. The braneworld paradigm [3] naturally arises in the context of supergravity and string theories and presents an alternative to Kaluza-Klein compactification of extra dimensions. The models formulated on AdS bulk provide a geometrical solution for the hierarchy problem between the electroweak and gravitational energy scales and also new perspectives and different interpretations for various problems in particle physics and cosmology.

In the Randall-Sundrum-type realizations of the braneworld models [4] the branes are parallel to the AdS boundary. Motivated by the radion stabilization and the generation of cosmological constant on branes, the Casimir effect in that setup has been widely investigated in the literature for scalar [5, 6], fermionic [7] and vector [8] fields. In the main part of the papers, as a physical characteristic of the vacuum, global quantities, such as the Casimir energy or the effective potential, are investigated by using various regularization schemes. Local observables carry more detailed information about the properties of the vacuum state. In particular, being a source of gravity in semiclassical Einstein equations, the vacuum expectation value (VEV) of the energy-momentum tensor is of special importance. It is investigated in [9, 10, 11] for scalar, fermionic and electromagnetic fields. The combined effects of a brane and topological defect of a cosmic string type on the local characteristics of the fermionic vacuum in AdS spacetime have been recently considered in [12]. For charged fields, another important local characteristic of the vacuum state, bilinear in the field, is the VEV of the current density. It has been studied in [13] for scalar and fermionic fields in the geometry of branes parallel to the boundary of locally AdS spacetime with a part of spatial dimensions compactified to a torus.

Motivated by an increase of interest to conformal field theories in the presence of boundaries (see, for example, references given in [14]), in recent studies the AdS/CFT correspondence is extended to the problems where boundaries are present in the conformal field theory side. In the corresponding setup the boundary CFT is dual to a theory in AdS bulk with additional boundaries intersecting the

AdS boundary at the locations of boundaries in CFT (AdS/BCFT correspondence) [15]. Problems with surfaces in the AdS bulk crossing the AdS boundary have been considered in recent studies of entanglement entropy in the context of AdS/CFT correspondence [16] (for reviews see [17, 18]). A geometric classical procedure is suggested for evaluation of the entanglement entropy of quantum systems living on the AdS boundary. In accordance of that procedure, the entanglement entropy for a bounded region in CFT is expressed in terms of the area of the minimal surface in the AdS bulk anchored at the boundary of that region.

In the papers cited above, the physical characteristics in the Casimir effect with branes serving as constraining boundaries, have been considered in the context of Randall-Sundrum-type models with branes parallel to the AdS boundary. Motivated by recent developments for physical models on AdS bulk with boundaries crossing the spacetime boundary and continuing the investigation started in [19], in the present paper we consider a problem with two branes orthogonal to the AdS boundary for a massive scalar field with general curvature coupling parameter. Though this problem is less symmetric than the setups with branes parallel to the AdS boundary, as it will be seen below, it is still exactly solvable.

The organization of the paper is as follows. In the next section we fix the problem setup and present the complete set of mode functions for a scalar field in the region between the branes. By using those functions, the positive frequency Wightman function is evaluated in Section 3. The brane-induced contribution is explicitly separated. Taking the coincidence limit of the arguments in that contribution, the mean field squared is investigated in Section 4. The behavior of the VEV in various asymptotic regions for the values of the parameters is discussed. Similar investigations for the VEV of the energy-momentum tensor are presented in Section 5. The Casimir forces acting on the branes are discussed in Section 6. It is shown that for Robin boundary conditions, in addition to the normal component, those forces have a nonzero component parallel to the branes (shear force). The nature of the forces is studied depending on the boundary conditions. The main results are summarized in Section 7. In Appendix A, by using a variant of the generalized Abel-Plana formula we provide an integral representation for the series in the mode-sum over the eigenvalues of the quantum number describing the degree of freedom along the direction normal to the branes.

## 2 Problem setup and the field modes

We consider a scalar field  $\varphi(x)$  on the background of a  $(D + 1)$ -dimensional AdS spacetime with the curvature radius  $\alpha$ . In Poincaré coordinates the corresponding line element is given by

$$ds^2 = g_{ik} dx^i dx^k = e^{-2y/\alpha} \left[ dt^2 - (dx^1)^2 - d\mathbf{x}^2 \right] - dy^2, \quad (2.1)$$

where the coordinates  $\mathbf{x} = (x^2, \dots, x^{D-1})$  are separated for the future convenience. In addition to the coordinate  $y$ ,  $-\infty < y < +\infty$ , we will also use the coordinate  $z$ , defined as  $z = \alpha e^{y/\alpha}$ ,  $0 < z < \infty$ , in terms of which the line element is written in a manifestly conformally flat form

$$ds^2 = \left( \frac{\alpha}{z} \right)^2 \left[ dt^2 - (dx^1)^2 - d\mathbf{x}^2 - dz^2 \right]. \quad (2.2)$$

The AdS boundary and horizon are presented by the hypersurfaces  $z = 0$  and  $z = \infty$ , respectively. The Ricci scalar and the cosmological constant are expressed in terms of the AdS curvature radius by the relations  $R = -D(D + 1)/\alpha^2$  and  $\Lambda = -D(D - 1)/(2\alpha^2)$ .

The operator of the scalar field with the curvature coupling constant  $\xi$  obeys the equation

$$\left( g^{ik} \nabla_i \nabla_k + m^2 + \xi R \right) \varphi(x) = 0. \quad (2.3)$$

The most popular special cases correspond to minimally and conformally coupled fields with  $\xi = 0$  and  $\xi = \xi_D = (D - 1)/(4D)$ , respectively. We are interested in the effects of two branes located at

$x^1 = a_1$  and  $x^1 = a_2$  on the local properties of vacuum state for the field  $\varphi(x)$  (see Figure 1). It is assumed that on the brane at  $x^1 = a_j$ ,  $j = 1, 2$ , the field obeys Robin boundary condition

$$(A_j + B_j n_j^i \nabla_i) \varphi(x) = 0, \quad (2.4)$$

where  $n_j^i$  is the normal to the brane. The discussion in what follows will be mainly focused on the VEVs in the region between the branes,  $a_1 \leq x^1 \leq a_2$ , with  $n_j^i = (-1)^{j-1} \delta_1^i z / \alpha$ . We will consider the special case with  $B_j/A_j = \alpha \beta_j / z$ , where  $\beta_j$ ,  $j = 1, 2$ , are constants. With this choice, the boundary condition (2.4) in the region between the branes is written as

$$(1 + (-1)^{j-1} \beta_j \partial_1) \varphi(x) = 0. \quad (2.5)$$

Note that for a given  $z$ , the physical coordinate that measures the proper distance from the branes is given by  $x_{(p)}^1 = \alpha x^1 / z$  and the condition (2.4) is presented as  $(1 + \beta_j n_j^1 \partial_{x_{(p)}^1}) \varphi(x) = 0$ . This means that the coefficient in the Robin boundary condition written in terms of the coordinate  $x_{(p)}^1$  is constant. The results for Dirichlet and Neumann boundary conditions are obtained in the special cases  $\beta_j = 0$  and  $\beta_j = \infty$ , respectively.

Our use of the term "brane" for the boundaries is, in some sense, conditional. Fundamental branes in string theory or phenomenological branes in braneworld scenarios are among the possible physical realizations of the boundary conditions (2.4). For example, in Randall-Sundrum type models they follow from the  $Z_2$ -symmetry with respect to the branes and the corresponding Robin coefficients are expressed in terms of constants in the brane mass terms of the part of the action located on the branes (see [6, 10]). The Robin conditions also arise on boundaries separating spatial regions with different geometries (this type of setup on the AdS bulk has been considered in [11] to model the finite thickness of branes). In this case the Robin coefficients are expressed in terms of geometric characteristics of the contacting regions. The Robin type boundary conditions were used to model the finite penetration of the field into the boundary with the penetration length determined by the coefficient in the boundary condition.

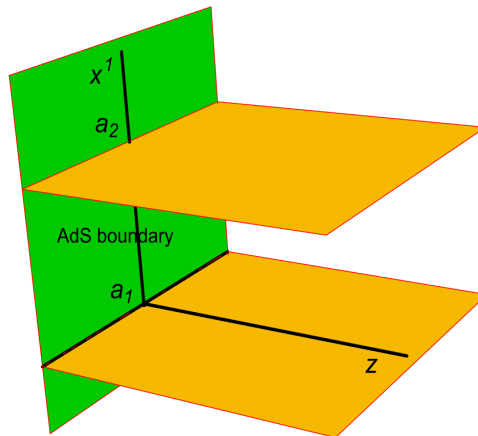


Figure 1: The geometry of the problem with branes intersecting the AdS boundary.

The properties of the vacuum state in the problem under consideration are encoded in two-point functions. Those functions are presented in the form of sums over complete set of the field modes obeying the boundary conditions. Those modes for a scalar field in AdS spacetime when the branes

are absent are well known in the literature. We will denote by  $\lambda$  the quantum number corresponding to the coordinate  $x^1$ . For the problem at hand the corresponding solutions are found by combining the factors  $e^{i\lambda x^1}$  and  $e^{-i\lambda x^1}$  with the relative coefficient that will be determined from the boundary conditions. Denoting by  $\sigma$  the set of quantum numbers specifying the modes, in the region between the branes the mode functions are written in the form

$$\varphi_\sigma(x) = C_\sigma z^{D/2} J_\nu(\gamma z) \cos[\lambda|x^1 - a_j| + \alpha_j(\lambda)] e^{i\mathbf{k}\mathbf{x} - iEt}, \quad (2.6)$$

where  $J_\nu(u)$  is the Bessel function,  $\mathbf{k} = (k^2, \dots, k^{D-1})$ ,  $-\infty < k^l < +\infty$ ,  $0 \leq \lambda < +\infty$ , and the energy is expressed as

$$E = \sqrt{\lambda^2 + \mathbf{k}^2 + \gamma^2}. \quad (2.7)$$

In (2.6) and in what follows we use the notation

$$\nu = \sqrt{\frac{D^2}{4} - D(D+1)\xi + m^2\alpha^2}, \quad (2.8)$$

assuming that  $\nu \geq 0$ . This condition is dictated by the stability of the vacuum state [20]. With the mode functions (2.6) the set of quantum numbers is specified as  $\sigma = (\lambda, \mathbf{k}, \gamma)$ .

From the boundary condition at  $x^1 = a_j$  it follows that

$$e^{2i\alpha_j(\lambda)} = \frac{i\lambda\beta_j - 1}{i\lambda\beta_j + 1}. \quad (2.9)$$

We have  $\alpha_j(\lambda) = \pi/2$  and  $\alpha_j(\lambda) = 0$  for Dirichlet and Neumann conditions, respectively. The boundary condition on the second brane gives the equation that determines the eigenvalues for the quantum number  $\lambda$ :

$$(b_1 + b_2)u \cos u + (u^2 b_1 b_2 - 1) \sin u = 0, \quad (2.10)$$

where  $u = \lambda a$  and  $b_j = \beta_j/a$ . This eigenvalue equation is the same as the corresponding equation for two parallel plates in the Minkowski bulk, considered in [21]. As it has been discussed in [21], depending on the values of  $b_j$ , the equation (2.10) may have single or two purely imaginary roots with respect to  $u$ . In the presence of those roots and for the part of the modes with  $\mathbf{k}^2 + \gamma^2 < |u|^2/a^2$  the energy becomes imaginary which signals about the instability of the vacuum state. Note that here the situation is different from that in the corresponding problem on the Minkowski bulk. In the latter problem the mass enters in the expression for the energy, and for imaginary modes with  $|u|/a < m$  the energy is positive for all the modes and the vacuum is stable. To have a stable vacuum state, we will assume the values of the parameters  $b_1$  and  $b_2$  for which all the roots of the equation (2.10) are real. Those values belong to the region in the plane  $(b_1, b_2)$  given by  $\{b_1 + b_2 \geq 1, b_1 b_2 \leq 0\} \cup \{b_{1,2} \leq 0\}$  (see [21]). We will denote by  $u = u_n$ ,  $n = 1, 2, \dots$ , the positive roots of the equation (2.10). For the eigenvalues of the quantum number  $\lambda$  one has  $\lambda = \lambda_n = u_n/a$ . For Dirichlet and Neumann boundary conditions the eigenvalue equation is reduced to  $\sin u = 0$  with the modes  $\lambda_n = \pi n/a$ , where  $n = 1, 2, \dots$ , and  $n = 0, 1, 2, \dots$ , for the first and second cases, respectively. Note the presence of an additional zero mode for Neumann condition. For Dirichlet condition on one brane and the Neumann one on another from (2.10) we get  $\cos u = 0$  and  $\lambda_n = \pi(n - 1/2)/a$ ,  $n = 1, 2, \dots$ .

The constant  $C_\sigma$  in (2.6) is determined from the normalization condition

$$\int d^D x \sqrt{|g|} g^{00} \varphi_\sigma(x) \varphi_{\sigma'}^*(x) = \frac{\delta_{nn'}}{2E} \delta(\mathbf{k} - \mathbf{k}') \delta(\gamma - \gamma'). \quad (2.11)$$

For the mode functions (2.6) this gives

$$|C_\sigma|^2 = \frac{(2\pi)^{2-D} \gamma}{\alpha^{D-1} a E N_n}, \quad (2.12)$$

with the notation

$$N_n = 1 + \frac{\sin u_n}{u_n} \cos [u_n + 2\alpha_j(\lambda_n)]. \quad (2.13)$$

Note that  $\cos [u_n + 2\alpha_1(\lambda_n)] = \cos [u_n + 2\alpha_2(\lambda_n)]$ . Having fixed the complete set of modes we pass to the evaluation of the Wightman function.

### 3 Wightman function

As a two-point function we consider the positive frequency Wightman function defined as the VEV  $W(x, x') = \langle 0 | \varphi(x) \varphi(x') | 0 \rangle$ . Expanding the operators  $\varphi(x)$  and  $\varphi(x')$  in terms of the complete set  $\{\varphi_\sigma(x), \varphi_\sigma^*(x)\}$  and using the definition of the vacuum state, it is written in the form of the following sum over the modes:

$$W(x, x') = \int_0^\infty d\gamma \int d\mathbf{k} \sum_{n=1}^\infty \varphi_\sigma(x) \varphi_\sigma^*(x'). \quad (3.1)$$

The problem is homogeneous in the subspace  $(t, \mathbf{x})$  and we expect that the dependence on the arguments in that subspace will enter in the form of the differences  $\Delta t = t - t'$  and  $\Delta \mathbf{x} = \mathbf{x} - \mathbf{x}'$ . Substituting the functions (2.6) and the expression (2.12) for the normalization coefficient, the Wightman function is expressed as

$$W(x, x') = \frac{2(zz')^{D/2}}{(2\pi\alpha)^{D-1}a} \int d\mathbf{k} e^{i\mathbf{k}\Delta\mathbf{x}} \int_0^\infty d\gamma \gamma J_\nu(\gamma z) J_\nu(\gamma z') S(b, \Delta t, x^1, x'^1), \quad (3.2)$$

where  $b = \sqrt{\gamma^2 + \mathbf{k}^2}$ , and

$$S(b, \Delta t, x^1, x'^1) = \pi \sum_{n=1}^\infty \frac{e^{-i\sqrt{\lambda_n^2 + b^2}\Delta t}}{\sqrt{\lambda_n^2 + b^2} N_n} \cos [\lambda_n |x^1 - a_j| + \alpha_j(\lambda_n)] \cos [\lambda_n |x'^1 - a_j| + \alpha_j(\lambda_n)]. \quad (3.3)$$

An equivalent representation for the series over  $n$  is obtained by using the definition (2.9) for the function  $\alpha_j(\lambda)$ :

$$S(b, \Delta t, x^1, x'^1) = \frac{\pi}{4} \sum_{n=1}^\infty \frac{e^{-i\sqrt{\lambda_n^2 + b^2}\Delta t}}{\sqrt{\lambda_n^2 + b^2} N_n} \left[ 2 \cos(\lambda_n \Delta x^1) + \sum_{l=\pm 1} \left( e^{i\lambda_n |x^1 + x'^1 - 2a_j|} \frac{i\lambda\beta_j - 1}{i\lambda\beta_j + 1} \right)^l \right]. \quad (3.4)$$

For boundary conditions different from Dirichlet or Neumann ones on both the branes, the eigenvalues  $\lambda_n$  are given implicitly, as roots of (2.10), and the representation (3.2) with (3.3) or (3.4) is not convenient for the investigation of the local VEVs in the coincidence limit.

In order to get around this inconvenience and also to separate explicitly the divergence in the coincidence limit, the integral representation (A.7) for the function (3.4) is obtained in Appendix A by using the generalized Abel-Plana formula from [22]. Substituting (A.7) in (3.2), the Wightman function is decomposed as

$$\begin{aligned} W(x, x') &= W_j(x, x') + \frac{(zz')^{D/2}}{(2\pi\alpha)^{D-1}} \int d\mathbf{k} e^{i\mathbf{k}\Delta\mathbf{x}} \int_0^\infty d\gamma \gamma J_\nu(\gamma z) J_\nu(\gamma z') \\ &\quad \times \int_b^\infty d\lambda \frac{\cosh(\sqrt{\lambda^2 - b^2}\Delta t)}{\sqrt{\lambda^2 - b^2}} \frac{2 \cosh(\lambda x_-^1) + \sum_{l=\pm 1} \left[ e^{l|x_+^1 - 2a_j|} c_j(\lambda) \right]^l}{c_1(\lambda) c_2(\lambda) e^{2a\lambda} - 1}, \end{aligned} \quad (3.5)$$

where and in what follows  $x_\pm^1 = x^1 \pm x'^1$  and

$$c_j(\lambda) = \frac{\beta_j \lambda - 1}{\beta_j \lambda + 1}. \quad (3.6)$$

Note that  $c_j(\lambda) = \tilde{c}_j(\lambda a)$ , with the functions  $\tilde{c}_j(u)$  defined in Appendix A after formula (A.1). In (3.5) we have defined the two-point function

$$W_j(x, x') = W_0(x, x') + \frac{(zz')^{\frac{D}{2}}}{(2\pi\alpha)^{D-1}} \int d\mathbf{k} e^{i\mathbf{k}\Delta\mathbf{x}} \int_0^\infty d\gamma \gamma J_\nu(\gamma z) J_\nu(\gamma z') \\ \times \int_b^\infty d\lambda \frac{\cosh(\sqrt{\lambda^2 - b^2}\Delta t)}{\sqrt{\lambda^2 - b^2}} \frac{e^{-\lambda x_+^1 - 2a_j|\lambda}}{c_j(\lambda)}. \quad (3.7)$$

Here, the part  $W_0(x, x')$  comes from the term  $S_0(b, \Delta t, x_\perp^1)$  in (A.4) and is given by

$$W_0(x, x') = \frac{(zz')^{\frac{D}{2}}}{2(2\pi\alpha)^{D-1}} \int d\mathbf{K} e^{i\mathbf{K}\Delta\mathbf{X}} \int_0^\infty d\gamma \gamma J_\nu(\gamma z) J_\nu(\gamma z') \frac{e^{-i\sqrt{\gamma^2 + \mathbf{K}^2}\Delta t}}{\sqrt{\gamma^2 + \mathbf{K}^2}}, \quad (3.8)$$

with  $\mathbf{X} = (x^1, \mathbf{x})$ ,  $\mathbf{K} = (k^1, k^2, \dots, k^{D-1})$ . The integration over the angular coordinates of the vector  $\mathbf{k}$  in (3.5) and (3.7) (and in a similar way for (3.8)) can be done by using the formula

$$\int d\mathbf{k} e^{i\mathbf{k}\Delta\mathbf{x}} g(k) = \frac{(2\pi)^{\frac{D}{2}-1}}{|\Delta\mathbf{x}|^{\frac{D}{2}-2}} \int_0^\infty dk k^{\frac{D}{2}-1} J_{\frac{D}{2}-2}(k|\Delta\mathbf{x}|) g(k), \quad (3.9)$$

for a given function  $g(k)$ , where  $k = |\mathbf{k}|$ .

The separate terms in (3.5) and (3.7) have clear physical interpretation. The function  $W_0(x, x')$  is the Wightman function in AdS spacetime in the absence of the branes. Its expression in terms of the hypergeometric function is well known from the literature (see below). As it has been mentioned in Appendix A, the last term in (3.5) vanishes in the limit  $(-1)^{j'} a_{j'} \rightarrow +\infty$ , where  $j' = 1$  for  $j = 2$  and  $j' = 2$  for  $j = 1$ . Hence, the function  $W_j(x, x')$  corresponds to the Wightman function in the problem with a single brane at  $x^1 = a_j$ . It has been obtained in [19]. The last term in (3.5) is interpreted as a contribution induced by the second brane at  $x^1 = a_{j'}$  when we add it to the geometry with a brane at  $x^1 = a_j$ . The representation of the Wightman function with combined contributions from the branes is obtained from (A.8):

$$W(x, x') = W_0(x, x') + \frac{(zz')^{\frac{D}{2}}}{(2\pi\alpha)^{D-1}} \int d\mathbf{k} e^{i\mathbf{k}\Delta\mathbf{x}} \int_0^\infty d\gamma \gamma J_\nu(\gamma z) J_\nu(\gamma z') \\ \times \int_b^\infty d\lambda \frac{\cosh(\sqrt{\lambda^2 - b^2}\Delta t)}{\sqrt{\lambda^2 - b^2}} \frac{2 \cosh(\lambda x_\perp^1) + \sum_{j=1,2} e^{|\lambda x_+^1 - 2a_j|\lambda} c_j(\lambda)}{c_1(\lambda) c_2(\lambda) e^{2a\lambda} - 1}. \quad (3.10)$$

For the angular part of the integral over  $\mathbf{k}$  we can use the relation (3.9).

In the representations (3.5) and (3.10) the explicit knowledge of the eigenvalues  $\lambda_n$  is not required and they are well adapted for the investigation of local VEVs. Those representations give the Wightman function in the region between the branes. In the regions  $x^1 < a_1$  and  $x^1 > a_2$  the Wightman functions coincide with that for the problem with a single brane and they are given by (3.7) with  $j = 1$  and  $j = 2$  in the first and second regions respectively.

For the special cases of Dirichlet and Neumann boundary conditions we have  $c_j(\lambda) = -\delta_J$ , where  $J = D, N$  correspond to Dirichlet and Neumann boundary conditions with  $\delta_D = 1$ ,  $\delta_N = -1$ . The part with the exponential function is reduced to  $1/(e^{2a\lambda} - 1)$ . Presenting this function as the series  $\sum_{n=1}^\infty e^{-2na\lambda}$ , the integral over  $\lambda$  is expressed in terms of the modified Bessel function  $K_0(u)$  (see [23]). Next, we use the result (3.9) for the integral over the angular coordinates of  $k$ . The integral over  $k$  is expressed through the associated Legendre function  $Q_\beta^\mu(x)$  and the final expression reads

$$W(x, x') = W_0(x, x') + \frac{\alpha^{1-D}}{2^{\frac{D}{2} + \nu + 1} \pi^{\frac{D}{2}}} \sum_{n=1}^\infty \left[ \sum_{l=\pm 1} f_\nu(u_{l,n}^{(-)}) - \delta_J \sum_{j=1,2} f_\nu(u_{j,n}^{(+)}) \right], \quad (3.11)$$

with the notations

$$\begin{aligned} u_{l,n}^{(-)} &= 1 + \frac{(2nla - x_-^1)^2 + |\Delta\mathbf{x}|^2 + \Delta z^2 - \Delta t^2}{2zz'}, \\ u_{j,n}^{(+)} &= 1 + \frac{(2na - |x_+^1 - 2a_j|)^2 + |\Delta\mathbf{x}|^2 + \Delta z^2 - \Delta t^2}{2zz'}, \end{aligned} \quad (3.12)$$

and  $\Delta z = z - z'$ . In (3.11) we have defined the function

$$\begin{aligned} f_\nu(u) &= \frac{2^{\nu+\frac{1}{2}}}{\sqrt{\pi}} e^{-\frac{D-1}{2}\pi i} \frac{Q_{\nu-\frac{1}{2}}^{\frac{D-1}{2}}(u)}{(u^2-1)^{\frac{D-1}{4}}} \\ &= \frac{\Gamma(\nu + \frac{D}{2})}{\Gamma(\nu + 1) u^{\nu+\frac{D}{2}}} F\left(\frac{2+2\nu+D}{4}, \frac{2\nu+D}{4}; \nu+1; \frac{1}{u^2}\right), \end{aligned} \quad (3.13)$$

with  $F(a, b; c; x) \equiv {}_2F_1(a, b; c; x)$  being the hypergeometric function.

The Wightman function for a scalar field in the brane-free AdS spacetime is expressed in terms of the function  $f_\nu(u)$  as

$$W_0(x, x') = \frac{\alpha^{1-D} f_\nu(u_{0,0}^{(-)})}{2^{\frac{D}{2}+\nu+1} \pi^{\frac{D}{2}}}, \quad (3.14)$$

and the formula (3.11) presents the Wightman function in the region between the branes in the form of the image sum. In the spacetime region  $(x_-^1)^2 + |\Delta\mathbf{x}|^2 + \Delta z^2 > \Delta t^2$  one has the relation  $u_{0,0}^{(-)} = \cosh(\sigma(x, x')/\alpha)$  with  $\sigma(x, x')$  being the geodesic distance between the spacetime points  $x$  and  $x'$ . In the cases of Dirichlet and Neumann boundary conditions, the Wightman function for the geometry of a single brane at  $x^1 = a_j$  is obtained from (3.11) in the limit  $(-1)^{j'} a_{j'} \rightarrow +\infty$ . In the series over  $n$  the contribution of the term  $n = 1, j = j'$  survives only and we get the result obtained in [19]:

$$W_j(x, x') = W_0(x, x') - \frac{\delta_j \alpha^{1-D}}{2^{\frac{D}{2}+\nu+1} \pi^{\frac{D}{2}}} f_\nu\left(1 + \frac{|x_+^1 - 2a_j|^2 + |\Delta\mathbf{x}|^2 + \Delta z^2 - \Delta t^2}{2zz'}\right). \quad (3.15)$$

We can also consider the problem with Dirichlet boundary condition on the brane  $x^1 = a_1$  and Neumann condition on the second brane. In this case  $c_j(\lambda) = (-1)^j$  and the Wightman function is obtained in a way similar to the cases of Dirichlet and Neumann conditions on both the branes. It can be seen that the corresponding expression is obtained from (3.11) by the replacements (the replacement of  $\delta_j$  should be made after the summation sign  $\sum_{j=1,2}$ )

$$\sum_{n=1}^{\infty} \rightarrow \sum_{n=1}^{\infty} (-1)^n, \quad \delta_j \rightarrow (-1)^{j-1}. \quad (3.16)$$

In the regions  $x^1 < a_1$  and  $x^1 > a_2$  the Wightman functions for the Dirichlet-Neumann combination of boundary conditions are given by (3.15) with  $\delta_j = 1$  and  $\delta_j = -1$ , respectively.

## 4 VEV of the field squared

In this section we investigate the VEV of the field squared  $\langle 0|\varphi^2|0\rangle \equiv \langle\varphi^2\rangle$ . It is obtained taking the coincidence limit of the arguments in the Wightman function. Of course, that limit is divergent and a renormalization procedure is required to extract finite physical values. Here we are interested in the effects induced by the branes. For points outside the branes the local geometry is the same as that for



AdS spacetime without branes. The divergences in the coincidence limit are determined by the local geometrical characteristics and we conclude that for  $x^1 \neq a_j$ ,  $j = 1, 2$ , they are the same as in AdS spacetime. Having extracted the part in the Wightman function corresponding to the latter geometry (the function  $W_0(x, x')$ ), the renormalization is reduced to that for brane-free AdS spacetime. That procedure for the VEVs of the field squared and of the energy-momentum tensor is well investigated in the literature.

Taking the coincidence limit  $x' \rightarrow x$  in (3.10), the VEV of the field squared is presented as

$$\begin{aligned} \langle \varphi^2 \rangle &= \langle \varphi^2 \rangle_0 + \frac{2^{2-D} \alpha^{1-D} z^D}{\pi^{\frac{D}{2}} \Gamma\left(\frac{D}{2} - 1\right)} \int_0^\infty dk k^{D-3} \int_0^\infty d\gamma \gamma J_\nu^2(\gamma z) \\ &\times \int_b^\infty d\lambda \frac{2 + \sum_{j=1,2} e^{2|x^1 - a_j| \lambda} c_j(\lambda)}{[c_1(\lambda) c_2(\lambda) e^{2a\lambda} - 1] \sqrt{\lambda^2 - b^2}}, \end{aligned} \quad (4.1)$$

where  $\langle \varphi^2 \rangle_0$  is the renormalized VEV in AdS spacetime when the branes are absent. Because of the maximal symmetry of AdS geometry the part  $\langle \varphi^2 \rangle_0$  does not depend on the spacetime point and it is well investigated in the literature. For further transformation of the brane-induced contribution in (4.1), instead of  $\lambda$  we introduce a new integration variable  $\chi = \sqrt{\lambda^2 - b^2}$  and then pass to polar coordinates in the plane  $(k, \chi)$ . After integrating over the angular part one finds

$$\langle \varphi^2 \rangle = \langle \varphi^2 \rangle_0 + \frac{(2\sqrt{\pi}\alpha)^{1-D} z^D}{\Gamma\left(\frac{D-1}{2}\right)} \int_0^\infty dr r^{D-2} \int_0^\infty d\gamma \frac{\gamma}{\lambda} \frac{2 + \sum_{j=1,2} e^{2|x^1 - a_j| \lambda} c_j(\lambda)}{c_1(\lambda) c_2(\lambda) e^{2a\lambda} - 1} J_\nu^2(\gamma z), \quad (4.2)$$

where  $\lambda = \sqrt{\gamma^2 + r^2}$ . Introducing polar coordinates in the plane  $(r, \gamma)$ , for the angular integral we use the result [24]

$$\int_0^1 dx x (1-x^2)^{\mu-3/2} J_\nu^2(ux) = \frac{\Gamma(\mu - 1/2)}{2^{2\nu+1}} u^{2\nu} F_\nu^\mu(u), \quad (4.3)$$

with the function

$$F_\nu^\mu(u) = \frac{{}_1F_2\left(\nu + \frac{1}{2}; \mu + \nu + \frac{1}{2}, 1 + 2\nu; -u^2\right)}{\Gamma(\mu + \nu + \frac{1}{2}) \Gamma(1 + \nu)}. \quad (4.4)$$

Here,  ${}_1F_2(a; b, c; z)$  is the hypergeometric function. The final expression reads

$$\langle \varphi^2 \rangle = \langle \varphi^2 \rangle_0 + \frac{(\sqrt{\pi}\alpha)^{1-D}}{2^{D+2\nu}} \int_0^\infty dx x^{D+2\nu-1} F_\nu^{D/2}(x) \frac{2 + \sum_{j=1,2} e^{2|x^1 - a_j| x/z} c_j(x/z)}{c_1(x/z) c_2(x/z) e^{2ax/z} - 1}. \quad (4.5)$$

In a similar way, by making use of the formula (3.5), we can obtain the representation

$$\langle \varphi^2 \rangle = \langle \varphi^2 \rangle_j + \frac{(\sqrt{\pi}\alpha)^{1-D}}{2^{D+2\nu}} \int_0^\infty dx x^{D+2\nu-1} F_\nu^{D/2}(x) \frac{2 + \sum_{l=\pm 1} \left[ e^{2|x^1 - a_j| x/z} c_j(x/z) \right]^l}{c_1(x/z) c_2(x/z) e^{2ax/z} - 1}, \quad (4.6)$$

where the VEV in the geometry of a single brane at  $x^1 = a_j$  is expressed as (see [19])

$$\langle \varphi^2 \rangle_j = \langle \varphi^2 \rangle_0 + \frac{(\sqrt{\pi}\alpha)^{1-D}}{2^{D+2\nu}} \int_0^\infty dx x^{D+2\nu-1} F_\nu^{D/2}(x) \frac{e^{-2|x^1 - a_j| x/z}}{c_j(x/z)}. \quad (4.7)$$

Note that the product  $\alpha^{D-1} \langle \varphi^2 \rangle$  depends on the quantities having dimension of length ( $x^1$ ,  $a_j$ ,  $\beta_j$ ) and on the coordinate  $z$  through the ratios  $x^1/z$ ,  $a_j/z$ ,  $\beta_j/z$ . Those ratios are the proper values of the quantities measured by an observer with fixed  $z$  in units of the curvature radius  $\alpha$ . This feature is a consequence of the AdS maximal symmetry.

For a conformally coupled massless field one has  $\nu = 1/2$  and

$$F_{1/2}^\mu(u) = \frac{2}{\sqrt{\pi}u^2} \left[ \frac{1}{\Gamma(\mu)} - \frac{J_{\mu-1}(2u)}{u^{\mu-1}} \right]. \quad (4.8)$$

For the VEV of the field squared this gives

$$\langle \varphi^2 \rangle = \langle \varphi^2 \rangle_0 + (z/\alpha)^{D-1} \langle \varphi^2 \rangle_{(M)}, \quad (4.9)$$

where

$$\langle \varphi^2 \rangle_{(M)} = \frac{1}{2^D \pi^{\frac{D}{2}}} \int_0^\infty d\lambda \lambda^{D-2} \left[ \frac{1}{\Gamma(D/2)} - \frac{J_{D/2-1}(2z\lambda)}{(z\lambda)^{D/2-1}} \right] \frac{2 + \sum_{j=1,2} e^{2|x^1 - a_j|\lambda} c_j(\lambda)}{c_1(\lambda)c_2(\lambda)e^{2a\lambda} - 1}. \quad (4.10)$$

The background geometry under consideration is conformally flat and the last term in (4.9) exhibits the standard conformal relation between the boundary-induced parts of the VEVs in two conformally related problems (see, for example, [25]). The geometry of two branes in AdS spacetime is conformally connected to the problem in the Minkowski spacetime with the line element

$$ds_M^2 = dt^2 - (dx^1)^2 - d\mathbf{x}^2 - dz^2, \quad (4.11)$$

involving two parallel Robin plates at  $x^1 = a_1$  and  $x^1 = a_2$  intersected by the plate  $z = 0$  with Dirichlet boundary condition. The latter plate is the conformal image of the AdS boundary. Note that the part in (4.10) coming from the first term in the square brackets gives the mean field squared in the region between two parallel plates in the Minkowski spacetime (the boundary at  $z = 0$  is absent) and the part with the second term is induced by the Dirichlet plate at  $z = 0$ .

Note that the Dirichlet boundary condition at  $z = 0$  in the conformally related problem on the Minkowski bulk is related to the condition we have imposed for the scalar modes (2.6) on the AdS boundary. For the values of the parameter  $\nu$  in the range  $0 \leq \nu < 1$  the general normalizable solution of the field equation has the form (2.6) with the Bessel function replaced by the linear combination  $J_\nu(\gamma z) + b_\sigma Y_\nu(\gamma z)$ , where  $Y_\nu(x)$  is the Neumann function. In this case an additional boundary condition is required on the AdS boundary for unique fixation of the set of modes. Our choice in (2.6) corresponds to Dirichlet condition. In the literature the Neumann and more general Robin boundary conditions have been considered as well (for recent discussions see [26]). In the conformally related problem on the Minkowski spacetime, the boundary condition on the  $z = 0$  image is determined by the respective condition on the AdS boundary. Note that the different boundary conditions will correspond to different conformal field theories in the context of the AdS/CFT correspondence.

Let us consider the Minkowskian limit of the problem at hand. It corresponds to the limit  $\alpha \rightarrow \infty$  for fixed value of the coordinate  $y$  in (2.1). Introducing in (4.5) a new integration variable  $\lambda = x/z$  and by taking into account that in the limit under consideration  $z \approx \alpha$  and  $\nu \approx m\alpha$ , we see that both the argument and the order  $\nu$  of the function  $F_\nu^{D/2}(\lambda z)$  are large. The uniform asymptotic expansion is obtained in [19] by using the corresponding expansion for the Bessel function in (4.3). It has been shown that for large  $\nu$  and  $\lambda < m$  the function  $F_\nu^{D/2}(\nu\lambda/m)$  is exponentially small. The VEV of the field squared is dominated by the contribution of the integral coming from the region  $\lambda > m$ . In that region the leading term in the expansion over  $1/\nu$  is given by [19]

$$F_\nu^\mu \left( \frac{\nu}{m} \lambda \right) \approx \frac{(\lambda^2 - m^2)^{\mu-1} (2m/\nu)^{2\nu+1}}{2\sqrt{\pi}\Gamma(D/2)\lambda^{2\mu+2\nu-1}}. \quad (4.12)$$

With this estimate we get  $\lim_{\alpha \rightarrow \infty} \langle \varphi^2 \rangle = \langle \varphi^2 \rangle_{(M)}^{(0)}$ , where

$$\langle \varphi^2 \rangle_{(M)}^{(0)} = \frac{(4\pi)^{-\frac{D}{2}}}{\Gamma(D/2)} \int_m^\infty d\lambda (\lambda^2 - m^2)^{D/2-1} \frac{2 + \sum_{j=1,2} e^{2|x^1 - a_j|\lambda} c_j(\lambda)}{c_1(\lambda)c_2(\lambda)e^{2a\lambda} - 1}, \quad (4.13)$$

is the mean field squared in the region between two Robin plates in background of Minkowski spacetime with the line element (4.11). This result for a massive field was presented in [22]. For a massless field it is reduced to the result derived in [21].

In order to find the mean field squared on AdS bulk in the special cases of Dirichlet and Neumann boundary conditions we can use the representation (3.11) for the Wightman function. The corresponding expression reads

$$\langle \varphi^2 \rangle = \langle \varphi^2 \rangle_0 + \frac{\alpha^{1-D}}{2^{\frac{D}{2}+\nu+1}\pi^{\frac{D}{2}}} \sum_{n=1}^{\infty} \left[ 2f_{\nu}(u_n) - \delta_J \sum_{j=1,2} f_{\nu}(u_{j,n}) \right], \quad (4.14)$$

with the notations

$$\begin{aligned} u_n &= 1 + 2(na/z)^2, \\ u_{j,n} &= 1 + \frac{2}{z^2} (na - |x^1 - a_j|)^2. \end{aligned} \quad (4.15)$$

An alternative representation is obtained from (4.5) expanding the function  $1/(e^{2ax/z} - 1)$ . The integral is evaluated by using the formula from [27]:

$$\int_0^{\infty} dx x^{2\mu+2\nu-1} e^{-2cx} F_{\nu}^{\mu}(x) = \frac{h_{\nu}^{\mu}(c)}{2\sqrt{\pi}}, \quad (4.16)$$

where the function in the right-hand side is defined as

$$h_{\nu}^{\mu}(u) = \frac{\Gamma(\mu + \nu)}{\Gamma(\nu + 1)} \frac{1}{u^{2(\mu+\nu)}} F\left(\nu + \frac{1}{2}, \mu + \nu; 1 + 2\nu; -\frac{1}{u^2}\right). \quad (4.17)$$

The VEV is presented as

$$\langle \varphi^2 \rangle = \langle \varphi^2 \rangle_0 + \frac{\alpha^{1-D}}{2^{D+2\nu+1}\pi^{\frac{D}{2}}} \sum_{n=1}^{\infty} \left[ 2h_{\nu}^{\frac{D}{2}}\left(\frac{na}{z}\right) - \delta_J \sum_{j=1,2} h_{\nu}^{\frac{D}{2}}\left(\frac{na - |x^1 - a_j|}{z}\right) \right]. \quad (4.18)$$

By employing the linear and quadratic transformation formulas for the hypergeometric function (see, for example, [28]) we can see that

$$h_{\nu}^{\frac{D}{2}}(x) = 2^{\frac{D}{2}+\nu} f_{\nu}(1 + 2x^2). \quad (4.19)$$

This relation shows the equivalence of the representations (4.14) and (4.18). Note that for a conformally coupled massless field

$$h_{1/2}^{\mu}(x) = \frac{4\Gamma(\mu + 1/2)}{\sqrt{\pi}(2\mu - 1)} \left[ x^{1-2\mu} - (x^2 + 1)^{\frac{1}{2}-\mu} \right]. \quad (4.20)$$

For Dirichlet or Neumann boundary conditions, the VEV in the problem with a single brane is obtained from (4.18) taking the limit  $a_1 \rightarrow -\infty$  or  $a_2 \rightarrow +\infty$ :

$$\langle \varphi^2 \rangle_j = \langle \varphi^2 \rangle_0 - \frac{\delta_J \alpha^{1-D}}{2^{D+2\nu+1}\pi^{\frac{D}{2}}} h_{\nu}^{\frac{D}{2}}\left(\frac{|x^1 - a_j|}{z}\right). \quad (4.21)$$

In problems with two scalar fields with Dirichlet and Neumann conditions on a single brane, the brane-induced mean field squared vanishes as a result of cancelations of contributions from Dirichlet and Neumann scalars. In particular, for  $D = 3$ , the electromagnetic field with perfectly conducting boundary condition on the brane is reduced to two scalar modes with Dirichlet and Neumann conditions

and their contributions in the vacuum energy density cancel each other. An equivalent representation for the single brane mean field squared  $\langle\varphi^2\rangle_j$ , given in [19], is derived from (3.15) in the coincidence limit. In (4.14) and (4.18), the parts corresponding to the contribution of the brane at  $x^1 = a_{j'}$ , when the second brane is absent, are presented by the term  $n = 1, j = 2$  for  $j' = 1$  and by the term  $n = 1, j = 1$  for  $j' = 2$ .

In the case of Dirichlet boundary condition on the brane  $x^1 = a_1$  and Neumann boundary condition on  $x^1 = a_2$  the expression for the mean field squared in the region between the branes is obtained from (4.18) making the replacements (3.16).

Now let us consider the behavior of the VEV  $\langle\varphi^2\rangle$  in asymptotic regions of the parameters. The VEV diverges on the branes. The divergences come from the single brane contributions: in the representation (4.6) the divergence at  $x^1 = a_j$  is contained in the part  $\langle\varphi^2\rangle_j$  (in the last term of (4.7)). Near the brane, for  $|x^1 - a_j| \ll z$ , the total VEV  $\langle\varphi^2\rangle$  is dominated by the last term in (4.7). Assuming additionally  $|x^1 - a_j| \ll |\beta_j|$  (non-Dirichlet boundary conditions), the leading term in the expansion over the distance from the brane reads [19]

$$\langle\varphi^2\rangle \approx \frac{\Gamma\left(\frac{D-1}{2}\right)}{(4\pi)^{\frac{D+1}{2}}} \left(\frac{z}{\alpha|x^1 - a_j|}\right)^{D-1}. \quad (4.22)$$

For the Dirichlet boundary condition the corresponding asymptotic differs from (4.22) by the sign of the right-hand side. The last term in the representation (4.6) is finite on the brane  $x^1 = a_j$ .

For points near the AdS boundary,  $z \ll |x^1 - a_j|$ ,  $j = 1, 2$ , the main contribution to the integral in (4.5) comes from the region with small values of  $x$ . By using the asymptotic expression  $F_\nu^\mu(x) \approx F_\nu^\mu(0)(1 + \mathcal{O}(x^2))$  with

$$F_\nu^\mu(0) = \frac{1}{\Gamma(\nu + 1)\Gamma(\mu + \nu + \frac{1}{2})}, \quad (4.23)$$

in the leading order, for the brane-induced contribution we get

$$\langle\varphi^2\rangle \approx \langle\varphi^2\rangle_0 + \frac{F_\nu^{\frac{D}{2}}(0)z^{D+2\nu}}{2^{D+2\nu}(\sqrt{\pi}\alpha)^{D-1}} \int_0^\infty d\lambda \lambda^{D+2\nu-1} \frac{2 + \sum_{j=1,2} e^{2|x^1 - a_j|\lambda} c_j(\lambda)}{c_1(\lambda)c_2(\lambda)e^{2a\lambda} - 1}. \quad (4.24)$$

Hence, for points near the AdS boundary and not too close to the branes, the brane-induced part in the mean field squared tends to zero like  $z^{D+2\nu}$ . For points near the horizon,  $z \gg a$ , the integral in (4.5) is dominated by the contribution coming from the region with large values of  $x$ . For those  $x$  one has [19]

$$F_\nu^\mu(x) \approx \frac{2^{2\nu}}{\sqrt{\pi}\Gamma(\mu)} x^{2\nu+1}, \quad x \gg 1, \quad (4.25)$$

and the VEV of the field squared is approximated by

$$\langle\varphi^2\rangle \approx \langle\varphi^2\rangle_0 + (z/\alpha)^{D-1} \langle\varphi^2\rangle_{(M)}^{(0)}|_{m=0}, \quad (4.26)$$

where  $\langle\varphi^2\rangle_{(M)}^{(0)}|_{m=0}$  (see (4.13)) is the corresponding VEV for a massless scalar field between two parallel plates in the Minkowski bulk with separation  $a$  [21]. Note that the latter is obtained from (4.10) in the limit  $z \rightarrow \infty$ . As seen, near the horizon the effects of the curvature on the brane-induced VEV are weak. Note that for a given  $a$  and large  $z$  the proper separation between the branes is much smaller than the curvature radius,  $a_p = \alpha a/z \ll \alpha$ , and the main contribution to the brane-induced VEV comes from the vacuum fluctuations with the wavelengths much smaller than the curvature radius. The influence of the gravitational field on those fluctuations is weak.

In Figure 2 the brane-induced VEV of the field squared,  $\langle\varphi^2\rangle_b = \langle\varphi^2\rangle - \langle\varphi^2\rangle_0$ , is plotted in the region between the branes as a function of the proper distance from the brane at  $x^1 = 0$  (in units of the AdS curvature radius  $\alpha$ ). For the location of the second brane we have taken  $a_2/z = 5$ . The graphs

are plotted for  $D = 4$  conformally (left panel) and minimally (right panel) coupled massive scalar fields with  $m\alpha = 0.5$ . The same boundary conditions are imposed on the branes ( $\beta_1 = \beta_2$ ) and the numbers near the curves indicate the respective values of the ratio  $\beta_1/z$ . The graphs for Dirichlet and Neumann boundary conditions are presented as well (Dir and Neu, respectively). The brane-induced mean field squared is negative for the Dirichlet case and positive for the Neumann one. For Robin conditions with sufficiently small values of  $|\beta_j|/z$ , the VEV is positive near the branes and negative in the region near the center with respect to the branes. With increasing  $|\beta_j|/z$ , started from some critical value, the VEV  $\langle\varphi^2\rangle_b$  becomes positive everywhere in the region between the branes. For the example presented in Figure 2, for the critical values one has  $\beta_j/z \approx -1.08$  and  $\beta_j/z \approx -0.70$  for conformally and minimally coupled scalars, respectively. The critical value for  $|\beta_j|/z$  decreases with decreasing  $a/z$ .

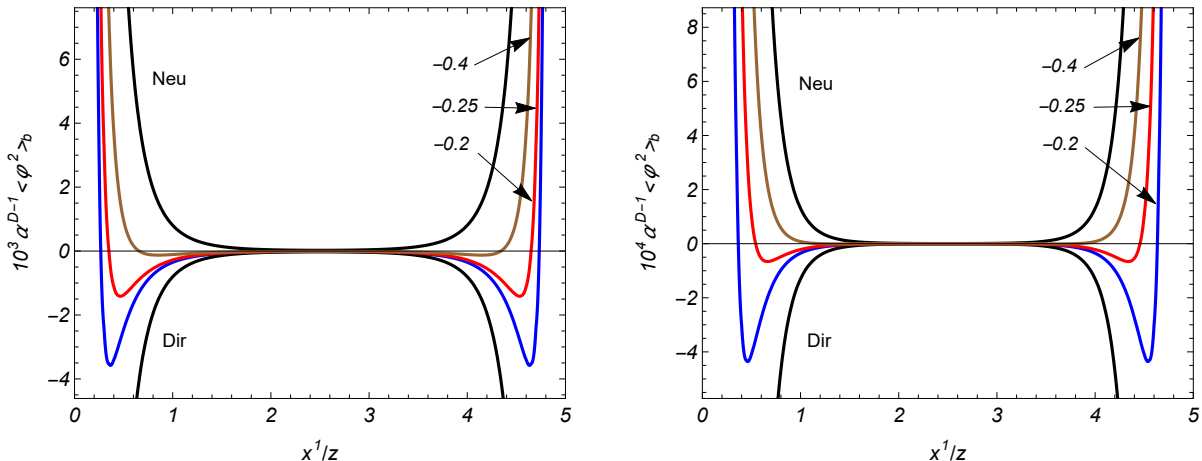


Figure 2: The brane-induced mean field squared in the region between the branes as a function of the ratio  $x^1/z$  for  $D = 4$  fields with conformal and minimal couplings (left and right panels, respectively). The graphs are plotted for  $m\alpha = 0.5$  and the numbers near the curves correspond to the values of the ratio  $\beta_1/z = \beta_2/z$ . The graphs for Robin boundary conditions are located in the region between the curves corresponding to Dirichlet and Neumann conditions.

## 5 Energy-momentum tensor

Another important characteristic of the vacuum state is the VEV of the energy-momentum tensor. With the known Wightman function and the VEV of the field squared, it is evaluated by using the formula

$$\langle T_{ik} \rangle = \frac{1}{2} \lim_{x' \rightarrow x} (\partial_i \partial'_k + \partial_k \partial'_i) W(x, x') + \hat{B}_{ik} \langle \varphi^2 \rangle, \quad (5.1)$$

where the operator acting on the VEV of the field squared is defined by

$$\hat{B}_{ik} = \left( \xi - \frac{1}{4} \right) g_{ik} g^{lm} \nabla_l \nabla_m - \xi (\nabla_i \nabla_k + R_{ik}), \quad (5.2)$$

with  $R_{ik} = -Dg_{ik}/\alpha^2$  being the Ricci tensor for AdS spacetime. In the geometry at hand one gets

$$\hat{B}_{00} = \left( \frac{1}{4} - \xi \right) \left( \partial_1^2 + \partial_z^2 - \frac{D-1}{z} \partial_z \right) - \frac{\xi}{z} \partial_z + \frac{D}{z^2} \xi, \quad (5.3)$$

and the spatial diagonal components are expressed as  $\hat{B}_{ll} = -\hat{B}_{00} - \hat{C}_{ll}$ ,  $l = 1, 2, \dots, D$ , where

$$\begin{aligned}\hat{C}_{11} &= \xi \partial_1^2, \quad \hat{C}_{ll} = 0, \quad l = 2, \dots, D-1, \\ \hat{C}_{DD} &= \xi \left( \partial_z^2 + \frac{2}{z} \partial_z \right).\end{aligned}\tag{5.4}$$

In addition to the diagonal components, the action of the operator (5.2) on  $\langle \varphi^2 \rangle$  gives a nonzero off-diagonal component  $\hat{B}_{1D} \langle \varphi^2 \rangle$  with the operator

$$\hat{B}_{1D} = -\xi \left( \partial_z + \frac{1}{z} \right) \partial_1.\tag{5.5}$$

By using the representation (3.10), the coincidence limit of the bitensor  $\partial_i \partial'_k W(x, x')$  is evaluated in a way we have described above for the mean field squared. For the diagonal components  $\langle T_{ll} \rangle$  with  $l \neq D$  the angular integrals at the last step are expressed in terms of the functions  $F_\nu^{D/2}(u)$  and  $F_\nu^{D/2+1}(u)$ . For the component  $\langle T_{DD} \rangle$  the integral is reduced to

$$\int_0^1 dx x (1-x^2)^{\frac{D-3}{2}} \left[ \partial_u \left( u^{\frac{D}{2}} J_\nu(ux) \right) \right]^2.\tag{5.6}$$

By making use of the equation for the Bessel function this integral is expressed in terms of the functions  $F_\nu^{D/2}(u)$ ,  $F_\nu^{D/2+1}(u)$  and of the first and second derivatives of  $F_\nu^{D/2}(u)$ .

After long but straightforward calculations, the VEVs of the diagonal components of the energy-momentum tensor are written in the form (no summation over  $i$ )

$$\begin{aligned}\langle T_i^i \rangle &= \langle T_i^i \rangle_0 - \frac{\alpha^{-1-D}}{2^{D+2\nu} \pi^{\frac{D-1}{2}}} \int_0^\infty dx x \left\{ \frac{E_i x^{D+2\nu} F_\nu^{\frac{D}{2}}(x)}{c_1(x/z) c_2(x/z) e^{2ax/z} - 1} \right. \\ &\quad \left. + \frac{2 + \sum_{j=1,2} e^{2|x^1 - a_j|x/z} c_j(x/z)}{c_1(x/z) c_2(x/z) e^{2ax/z} - 1} \left[ A_i x^{D+2\nu} F_\nu^{\frac{D}{2}+1}(x) + \hat{B}_i x^{D+2\nu} F_\nu^{\frac{D}{2}}(x) \right] \right\}.\end{aligned}\tag{5.7}$$

Here we have defined the operators

$$\begin{aligned}\hat{B}_1 &= \left( \xi - \frac{1}{4} \right) \partial_x^2 + \left[ \frac{D-1}{4} - (D-2)\xi \right] \frac{\partial_x}{x} - \frac{D\xi}{x^2}, \\ \hat{B}_i &= \hat{B}_1 + 4\xi - 1, \quad i = 0, 2, \dots, D-1, \\ \hat{B}_D &= \frac{1}{4} \partial_x^2 - D(\xi + \xi_D) \frac{\partial_x}{x} + \frac{D^2\xi - m^2\alpha^2}{x^2} + 4\xi,\end{aligned}\tag{5.8}$$

and the coefficients

$$\begin{aligned}E_i &= 2(1 - 4\xi), \quad i = 0, 2, \dots, D, \quad E_1 = -2, \\ A_i &= \frac{1}{2}, \quad i = 0, 2, \dots, D-1, \quad A_D = \frac{1-D}{2},\end{aligned}\tag{5.9}$$

and  $A_1 = 0$ . The nonzero off-diagonal component is expressed as

$$\langle T_D^1 \rangle = -\frac{2\alpha^{-1-D}}{2^{D+2\nu} \pi^{\frac{D-1}{2}}} \int_0^\infty dx \frac{\sum_{j=1,2} (-1)^j e^{2|x^1 - a_j|x/z} c_j(x/z)}{c_1(x/z) c_2(x/z) e^{2ax/z} - 1} \left[ \left( \xi - \frac{1}{4} \right) x \partial_x + \xi \right] x^{D+2\nu} F_\nu^{\frac{D}{2}}(x).\tag{5.10}$$

In (5.7), the part  $\langle T_i^k \rangle_0$  corresponds to the vacuum energy-momentum tensor in the brane-free AdS spacetime. Similar to the case of the VEV  $\langle \varphi^2 \rangle_0$ , that part is well-known from the literature. From the

maximal symmetry of the AdS geometry one has  $\langle T_i^k \rangle_0 = \text{const} \cdot \delta_i^k$ . The components  $\langle T_0^0 \rangle$  and  $\langle T_i^i \rangle$ ,  $i = 2, \dots, D-1$ , determining the energy density and stresses along the directions parallel to the branes (except the component  $i = D$ ), are equal. Of course, that is a consequence of the problem symmetry. As another consequence of the symmetry, the VEV of the energy-momentum tensor depends on the variables  $x^1, a_j, \beta_j, z$  in terms of the combinations  $x^1/z, a_j/z, \beta_j/z$ . The first and second derivatives of the product  $x^{D+2\nu} F_\nu^{D/2}(x)$ , appearing in (5.7) and (5.10), are expressed in terms of the functions  $F_\nu^{D/2}(x), F_\nu^{D/2-1}(x)$ , and  $F_\nu^{D/2-2}(x)$ . The corresponding relations can be found in [19].

Let us denote by  $\langle T_i^k \rangle_b = \langle T_i^k \rangle - \langle T_i^k \rangle_0$  the brane-induced contribution to the vacuum energy-momentum tensor. We can check the following relation for the corresponding trace:

$$\langle T_i^i \rangle_b = D(\xi - \xi_D) \nabla_l \nabla^l \langle \varphi^2 \rangle_b + m^2 \langle \varphi^2 \rangle_b, \quad (5.11)$$

where the brane-induced part in the VEV of the field squared is given by the last term in (4.5). The trace is zero for a conformally coupled massless field. Another relation expected from general arguments is the covariant conservation equation  $\nabla_k \langle T_i^k \rangle_b = 0$ . The latter is a necessary condition for  $\langle T_i^k \rangle_b$  to be a source in the Einstein field equations. From the equations with  $i = 1$  and  $i = D$  the following two relations are obtained between the separate components (see also [19] for the corresponding relations in the geometry of a single brane):

$$\begin{aligned} \partial_1 \langle T_1^1 \rangle_b &= -z^{D+1} \partial_z \left( \frac{\langle T_1^D \rangle_b}{z^{D+1}} \right), \\ \partial_1 \langle T_D^1 \rangle_b &= -z^D \partial_z \left( \frac{\langle T_D^D \rangle_b}{z^D} \right) - \frac{1}{z} \sum_{k=0}^{D-1} \langle T_k^k \rangle_b. \end{aligned} \quad (5.12)$$

The first equation shows that the dependence of the normal stress on the coordinate  $x^1$  is related to the presence of the nonzero off-diagonal component.

The VEV of the energy-momentum tensor in the geometry of a single brane at  $x^1 = a_j$  is obtained from (5.7) and (5.10) in the limit  $(-1)^{j'} a_{j'} \rightarrow \infty$  with  $j' \neq j$ . For the diagonal components this gives (no summation over  $i$ )

$$\langle T_i^i \rangle_j = \langle T_i^i \rangle_0 - \frac{\alpha^{-1-D}}{2^{D+2\nu} \pi^{\frac{D-1}{2}}} \int_0^\infty dx x \frac{e^{-2|x^1-a_j|x/z}}{c_j(x/z)} \left[ A_i x^{D+2\nu} F_\nu^{\frac{D}{2}+1}(x) + \hat{B}_i x^{D+2\nu} F_\nu^{\frac{D}{2}}(x) \right]. \quad (5.13)$$

The corresponding expression for the off-diagonal component reads

$$\langle T_D^1 \rangle_j = \frac{2(-1)^j \alpha^{-1-D}}{2^{D+2\nu} \pi^{\frac{D-1}{2}}} \int_0^\infty dx \frac{e^{-2|x^1-a_j|x/z}}{c_j(x/z)} \left[ \left( \xi - \frac{1}{4} \right) x \partial_x + \xi \right] x^{D+2\nu} F_\nu^{\frac{D}{2}}(x). \quad (5.14)$$

The formulae (5.13) and (5.14) were obtained in [19] from the Wightman function (3.7) by using (5.1). Note that (5.14) presents the VEV in the region  $x^1 > a_1$  for  $j = 1$  and in the region  $x^1 < a_2$  for  $j = 2$ . Making the replacement

$$(-1)^j \rightarrow \text{sgn}(a_j - x^1), \quad (5.15)$$

in (5.14) we obtain the expression for a single brane at  $x^1 = a_j$  that is valid for both regions  $x^1 < a_j$  and  $x^1 > a_j$ .

Extracting the single brane contributions from the VEVs we can obtain the following equivalent representations for the components of the vacuum energy-momentum tensor (no summation over  $i$ ):

$$\begin{aligned} \langle T_i^i \rangle &= \langle T_i^i \rangle_j - \frac{\alpha^{-1-D}}{2^{D+2\nu} \pi^{\frac{D-1}{2}}} \int_0^\infty dx x \left\{ \frac{E_i x^{D+2\nu} F_\nu^{\frac{D}{2}}(x)}{c_1(x/z) c_2(x/z) e^{2ax/z} - 1} \right. \\ &\quad \left. + \frac{2 + \sum_{l=\pm 1} \left[ e^{2|x^1-a_j|x/z} c_j(x/z) \right]^l}{c_1(x/z) c_2(x/z) e^{2ax/z} - 1} \left[ A_i x^{D+2\nu} F_\nu^{\frac{D}{2}+1}(x) + \hat{B}_i x^{D+2\nu} F_\nu^{\frac{D}{2}}(x) \right] \right\}, \end{aligned} \quad (5.16)$$

and

$$\begin{aligned} \langle T_D^1 \rangle &= \langle T_D^1 \rangle_j - \frac{(-1)^j \alpha^{-1-D}}{2^{D+2\nu-1} \pi^{\frac{D-1}{2}}} \int_0^\infty dx \frac{\sum_{l=\pm 1} l \left[ e^{2|x^1-a_j|x/z} c_j(x/z) \right]^l}{c_1(x/z) c_2(x/z) e^{2ax/z} - 1} \\ &\times \left[ \left( \xi - \frac{1}{4} \right) x \partial_x + \xi \right] x^{D+2\nu} F_\nu^{\frac{D}{2}}(x). \end{aligned} \quad (5.17)$$

The last terms in these representations are the contributions induced by the brane at  $x^1 = a_j$  when we add it to the problem with a single brane at  $x^1 = a_j$ . Those terms are finite on the brane  $x^1 = a_j$  and the divergences on that brane come from the single brane contribution  $\langle T_i^k \rangle_j$ . For points near the brane the total VEV is dominated by the single brane contribution. Under the conditions  $|x^1 - a_j| \ll z, |\beta_j|$ , the corresponding leading terms in the expansion over the distance from the brane are given in [19]:

$$\langle T_0^0 \rangle_b \approx \frac{(1-D) \langle T_1^1 \rangle_b}{(|x^1 - a_j|/z)^2} \approx \frac{z \langle T_D^1 \rangle_b}{x^1 - a_j} \approx \frac{2D (\xi_D - \xi) \Gamma\left(\frac{D+1}{2}\right)}{\pi^{\frac{D+1}{2}} (2\alpha|x^1 - a_j|/z)^{D+1}}. \quad (5.18)$$

For Dirichlet boundary condition,  $\beta_j = 0$ , the leading terms are given by the same expressions with opposite signs. As seen, the divergence on the branes is weaker for the normal stress and off-diagonal component. For conformal coupling the leading terms vanish and the next terms in the expansion should be kept.

In the case of a conformally coupled massless field, by using the expression (4.8) for the function  $F_\nu^\mu(x)$ , the vacuum energy-momentum tensor is presented in the form

$$\langle T_k^i \rangle = \langle T_k^i \rangle_0 + (z/\alpha)^{D+1} \langle T_k^i \rangle_{(M)}, \quad (5.19)$$

where  $\langle T_i^k \rangle_{(M)}$  is the corresponding VEV in the region  $a_1 < x^1 < a_2$ ,  $z > 0$  for the geometry of plates at  $x^1 = a_1, a_2$  and  $z = 0$  in the Minkowski spacetime with the line element (4.11). On the plates  $x^1 = a_1, a_2$  the field obeys Robin boundary condition (2.5) and on the plate  $z = 0$  the Dirichlet boundary condition is imposed. For the diagonal components the Minkowskian VEV is given by (no summation over  $i$ )

$$\begin{aligned} \langle T_i^i \rangle_M &= \langle T_i^i \rangle_M^{(0)} + \frac{\pi^{-\frac{D}{2}}}{2^{D+1} D} \int_0^\infty d\lambda \frac{\lambda^D}{c_1(\lambda) c_2(\lambda) e^{2a\lambda} - 1} \left\{ a^{(i)} g_{\frac{D}{2}-1}(\lambda z) \right. \\ &\left. + \left[ 2 + \sum_{j=1,2} e^{2|x^1-a_j|\lambda} c_j(\lambda) \right] \left[ b^{(i)} g_{\frac{D}{2}-1}(\lambda z) + c^{(i)} g_{\frac{D}{2}}(\lambda z) \right] \right\}, \end{aligned} \quad (5.20)$$

with the coefficients

$$\begin{aligned} (a^{(0)}, a^{(1)}, a^{(D)}) &= (4, -4D, 4), \\ (b^{(0)}, b^{(1)}, b^{(D)}) &= (0, 2, -2), \\ (c^{(0)}, c^{(1)}, c^{(D)}) &= (1, 1 - D, 0). \end{aligned} \quad (5.21)$$

In (5.20) we have introduced the function

$$g_\mu(x) = x^{-\mu} J_\mu(2x), \quad (5.22)$$

and (no summation over  $i$ )

$$\langle T_i^k \rangle_M^{(0)} = -\delta_i^k \frac{(-D)^{\delta_i^1} (4\pi)^{-\frac{D}{2}}}{\Gamma\left(\frac{D}{2} + 1\right)} \int_0^\infty d\lambda \frac{\lambda^D}{c_1(\lambda) c_2(\lambda) e^{2a\lambda} - 1} \quad (5.23)$$



is the corresponding VEV in the problem where the plate  $z = 0$  is absent. Hence, the last term in (5.20) is induced by the Dirichlet plate  $z = 0$  added to the geometry of two parallel plates. For the off-diagonal component in the Minkowski bulk we obtain

$$\langle T_D^1 \rangle_{(M)} = \frac{2z^{1-\frac{D}{2}}}{2^{D+2\nu}\pi^{\frac{D}{2}}D} \int_0^\infty d\lambda \lambda^{\frac{D}{2}+1} \frac{\sum_{j=1,2} (-1)^j e^{2|x^1-a_j|\lambda} c_j(\lambda)}{c_1(\lambda)c_2(\lambda)e^{2a\lambda} - 1} J_{\frac{D}{2}}(2\lambda z). \quad (5.24)$$

For the VEV of the energy-momentum tensor, the consideration of the Minkowskian limit, corresponding to large values of the curvature radius  $\alpha$ , is similar to that for the mean field squared. By taking into account that both  $\nu$  and  $z$  are large, we use the asymptotic (4.12) for the functions  $F_\nu^{D/2}(x)$  and  $F_\nu^{D/2+1}(x)$  in (5.7) and (5.10). For the diagonal components, to the leading order over  $1/\alpha$  one gets  $\langle T_i^i \rangle \approx \langle T_i^i \rangle_{(M)}^{(0)}$ , where (no summation over  $i$ )

$$\begin{aligned} \langle T_i^i \rangle_{(M)}^{(0)} &= -\frac{(4\pi)^{-\frac{D}{2}}}{D\Gamma(D/2)} \int_m^\infty d\lambda \frac{(\lambda^2 - m^2)^{D/2}}{c_1(\lambda)c_2(\lambda)e^{2a\lambda} - 1} \\ &\times \left[ 2 + \frac{4D(\xi - \xi_D)w^2 - m^2}{\lambda^2 - m^2} \sum_{j=1,2} e^{2|x^1-a_j|\lambda} c_j(\lambda) \right], \end{aligned} \quad (5.25)$$

for the components  $i \neq 1$  and

$$\langle T_1^1 \rangle_{(M)}^{(0)} = \frac{2(4\pi)^{-\frac{D}{2}}}{\Gamma(D/2)} \int_m^\infty d\lambda \frac{\lambda^2 (\lambda^2 - m^2)^{D/2-1}}{c_1(\lambda)c_2(\lambda)e^{2a\lambda} - 1}, \quad (5.26)$$

for the normal stress. These results coincide with the expressions given in [22] for the VEV of the energy-momentum tensor between two plates in the Minkowski bulk. In the massless limit they are reduced to the expressions in [21]. Note that the distribution of the normal stress is uniform. For the off-diagonal component the leading order term in the expansion over  $1/\alpha$  is expressed as

$$\begin{aligned} \langle T_D^1 \rangle &\approx -\frac{2(4\pi)^{-\frac{D}{2}}}{\Gamma(D/2)\alpha} \int_m^\infty d\lambda \frac{\sum_{j=1,2} (-1)^j e^{2|x^1-a_j|\lambda} c_j(\lambda)}{c_1(\lambda)c_2(\lambda)e^{2a\lambda} - 1} \\ &\times \lambda (\lambda^2 - m^2)^{D/2-2} \left[ D(\xi - \xi_D) \lambda^2 - \left( 2\xi - \frac{1}{4} \right) m^2 \right]. \end{aligned} \quad (5.27)$$

Of course, this component vanishes in the Minkowskian limit.

Now let us consider the special cases of Dirichlet and Neumann boundary conditions. Similar to the discussion for the field squared, we expand the function  $1/(e^{2ax/z} - 1)$  in (5.7). The resulting integral over  $x$  is presented in terms of the integral (4.16) and its first and second order derivatives with respect to  $c$ . In this way we can show that the VEVs of the diagonal components of the energy-momentum tensor are presented as (no summation over  $i$ )

$$\langle T_i^i \rangle = \langle T_i^i \rangle_0 - \frac{\alpha^{-1-D}}{2^{D+2\nu}\pi^{\frac{D}{2}}} \sum_{n=1}^\infty \left\{ \left[ \frac{E_i}{8} \partial_c^2 h_\nu^{\frac{D}{2}}(c) + q_\nu^{(i)}(c) \right]_{c=\frac{na}{z}} - \frac{\delta_J}{2} \sum_{j=1,2} q_\nu^{(i)}(c) \Big|_{c=\frac{na-|x^1-a_j|}{z}} \right\}. \quad (5.28)$$

Here we have defined the function

$$q_\nu^{(i)}(c) = \left[ \left( w_2^{(i)} c^2 + w^{(i)} \right) \partial_c^2 + w_1^{(i)} c \partial_c + w_0^{(i)} \right] h_\nu^{\frac{D}{2}}(c) + A_i h_\nu^{\frac{D}{2}+1}(c), \quad (5.29)$$

with the coefficients

$$(w_2^{(i)}, w_1^{(i)}, w_0^{(i)}, w^{(i)}) = \left( \xi - \frac{1}{4}, D\xi - \frac{D+1}{4}, -D\xi, \left( \xi - \frac{1}{4} \right) \delta_1^i \right), \quad (5.30)$$

for  $i \neq D$  and

$$(w_2^{(D)}, w_1^{(D)}, w_0^{(D)}, w^{(D)}) = \left( \frac{1}{4}, D\xi + \frac{D+1}{4}, D^2\xi - m^2\alpha^2, \xi \right). \quad (5.31)$$

For the off-diagonal component we get

$$\langle T_D^1 \rangle = \frac{\delta_J \alpha^{-1-D}}{2^{D+2\nu+3} \pi^{\frac{D}{2}}} \sum_{n=1}^{\infty} \sum_{j=1,2} (-1)^j [(4\xi - 1) c \partial_c - 1] \partial_c h_\nu^{\frac{D}{2}}(c) \Big|_{c=\frac{na-|x^1-a_j|}{z}}. \quad (5.32)$$

This component has opposite signs for Dirichlet and Neumann boundary conditions. Note that for the system of two scalars with Dirichlet and Neumann boundary conditions and with the same mass the total energy-momentum tensor is diagonal and does not depend on the coordinate  $x^1$ .

The VEVs for a single brane with Dirichlet or Neumann boundary conditions are obtained from (5.28) in the limit when the location of the second brane tends to infinity. For the diagonal components this gives (no summation over  $i$ )

$$\langle T_i^i \rangle = \langle T_i^i \rangle_0 + \frac{\delta_J \alpha^{-1-D}}{2^{D+2\nu+1} \pi^{\frac{D}{2}}} q_\nu^{(i)} \left( \frac{|x^1 - a_j|}{z} \right). \quad (5.33)$$

In a similar way the expression for the off-diagonal component reads

$$\langle T_D^1 \rangle = \text{sgn}(x^1 - a_j) \frac{\delta_J \alpha^{-1-D}}{2^{D+2\nu+3} \pi^{\frac{D}{2}}} [(4\xi - 1) c \partial_c - 1] \partial_c h_\nu^{\frac{D}{2}}(c) \Big|_{c=|x^1-a_j|/z}. \quad (5.34)$$

Alternative representations for the VEVs (5.33) and (5.34) in terms of the function (3.13) are provided in [19].

The VEVs for the components of the energy-momentum tensor in the special case of Dirichlet boundary condition on the brane  $x^1 = a_1$  and Neumann condition on  $x^1 = a_1$  are obtained from (5.28) and (5.32) by the replacements (3.16).

Let us consider the behavior of the vacuum energy-momentum tensor near the AdS boundary and horizon. Near the AdS boundary, assuming that  $z \ll |x^1 - a_j|$  for  $j = 1, 2$ , the contributions of small  $x$  dominate in (5.7) and (5.10). To the leading order, making the replacement  $F_\nu^{\frac{D}{2}}(x) \approx F_\nu^{\frac{D}{2}}(0)$ , with  $F_\nu^{\frac{D}{2}}(0)$  given by (4.23), we get (no summation over  $i$ )

$$\begin{aligned} \langle T_i^i \rangle &\approx \langle T_i^i \rangle_0 - \frac{B_\nu F_\nu^{\frac{D}{2}}(0) z^{D+2\nu}}{2^{D+2\nu} \pi^{\frac{D-1}{2}} \alpha^{D+1}} [2\nu - (D+2\nu) \delta_i^D] \int_0^\infty d\lambda \lambda^{D+2\nu-1} \frac{2 + \sum_{j=1,2} e^{2|x^1-a_j|\lambda} c_j(\lambda)}{c_1(\lambda) c_2(\lambda) e^{2a\lambda} - 1}, \\ \langle T_D^1 \rangle &\approx -\frac{2B_\nu F_\nu^{\frac{D}{2}}(0) z^{D+2\nu+1}}{2^{D+2\nu} \pi^{\frac{D-1}{2}} \alpha^{D+1}} \int_0^\infty d\lambda \lambda^{D+2\nu} \frac{\sum_{j=1,2} (-1)^j e^{2|x^1-a_j|\lambda} c_j(\lambda)}{c_1(\lambda) c_2(\lambda) e^{2a\lambda} - 1}, \end{aligned} \quad (5.35)$$

where we have defined

$$B_\nu = (D+2\nu+1) \xi - \frac{D+2\nu}{4}. \quad (5.36)$$

Under the conditions assumed, all the components tend to zero in the limit  $z \rightarrow 0$ . Note that the coefficient  $B_\nu$  is negative for minimally and conformally coupled fields.

For points tending to the horizon the coordinate  $z$  is large. Assuming that  $z \gg a$  we use the asymptotic (4.25) for the function  $F_\nu^{\frac{D}{2}}(x)$ . For the diagonal components this gives (no summation over  $i$ )

$$\langle T_i^i \rangle \approx \langle T_i^i \rangle_0 + (z/\alpha)^{D+1} \langle T_i^i \rangle_{(M)}^{(0)} \Big|_{m=0}, \quad (5.37)$$

with  $\langle T_i^i \rangle_{(M)}^{(0)}$  being the corresponding VEV for two parallel plates in Minkowski spacetime given by (5.25) for a massive field. The leading term in the expansion of the off-diagonal component is obtained

from (5.27) taking  $m = 0$  and multiplying by  $(z/\alpha)^D$ . For a non-conformally coupled field it behaves like  $(z/\alpha)^D$ . For the conformal coupling the next term in the expansion should be kept.

Figure 3 presents the brane-induced energy density for conformally (left panel) and minimally (right panel) coupled scalar fields in the region between the branes versus the proper distance from the brane (in units of  $\alpha$ ). The graphs are plotted for  $a_1 = 0$ ,  $a_2/z = 5$ ,  $m\alpha = 0.5$  and for the same Robin boundary conditions on the branes ( $\beta_1 = \beta_2$ ). The numbers near the graphs correspond to the values of the ratio  $\beta_1/z$ . We have also plotted the graphs for Dirichlet and Neumann boundary conditions. In accordance with the asymptotic (5.18), for a minimally coupled field and for non-Dirichlet boundary conditions the vacuum energy density is positive near the branes. For Dirichlet boundary condition the energy density is negative. The behavior of the energy density near the center with respect to the branes depends on the Robin coefficients. For  $\beta_j/z < 0$  and sufficiently close to zero the brane-induced energy density is negative near the center. With increasing value of  $|\beta_j|/z$ , started from certain critical value  $\beta_j^{(c)}$ , that depends on  $a/z$ , it becomes positive everywhere in the region between the branes. For the values of the parameters corresponding to Figure 3, the critical values are given by  $\beta_j^{(c)}/z \approx -1.12$  and  $\beta_j^{(c)}/z \approx -0.69$  in the cases of conformal and minimal couplings, respectively. The critical values  $|\beta_j^{(c)}|/z$  are increasing functions of  $a/z$ .

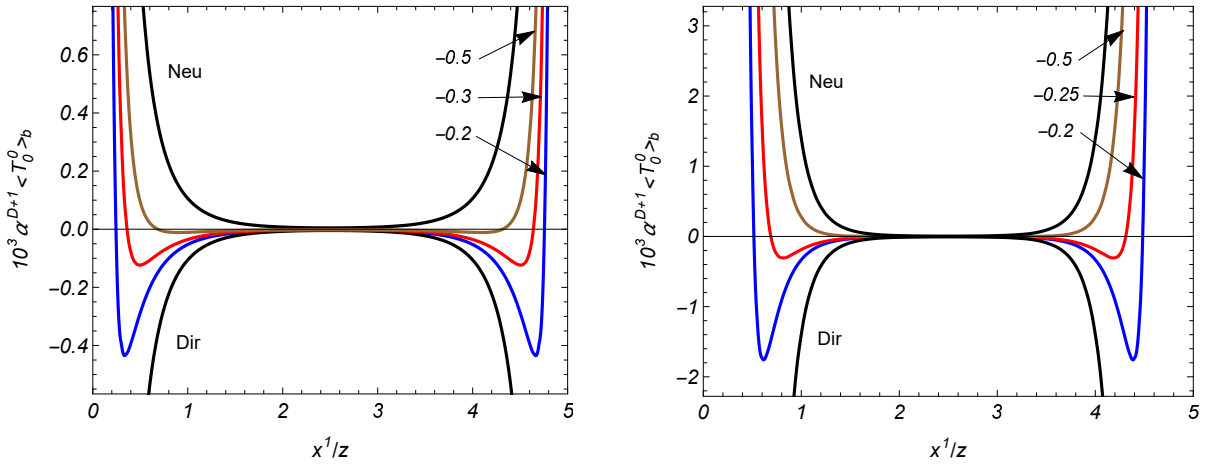


Figure 3: The vacuum energy densities for  $D = 4$  conformally (left panel) and minimally (right panel) coupled scalar fields induced by the branes in the region  $0 < x^1/z < 5$ . The graphs are plotted in the cases of Dirichlet, Neumann and Robin boundary conditions (with the values of  $\beta_1/z = \beta_2/z$  given near the curves) for the locations of the branes  $a_1 = 0$ ,  $a_2/z = 5$  and for  $m\alpha = 0.5$ .

In this section we have considered the local densities induced by the branes. They are well defined for points away from the branes and do not contain renormalization ambiguities. The global quantities, such as the total vacuum energy in the region between the branes (per unit surface of the branes), are also of physical interest. However, because of the surface divergences, it cannot be obtained by direct integration of the vacuum energy density: an additional renormalization is required. This problem is well-known from the theory of the Casimir effect for curved boundaries in flat spacetime. It is worth mentioning that for general Robin boundary conditions the vacuum energy obtained by the integration of the bulk energy density, in general, does not coincide with the total vacuum energy evaluated as the sum of the ground state energies for elementary oscillators. As it has been discussed in [29] for general case of the bulk and boundary geometries, the reason for that is the presence of surface energy density located on constraining boundaries. For a scalar field with general curvature coupling parameter the expression for the surface energy-momentum tensor is obtained in [29] by using the standard variational procedure. Similar to the case of the integrated bulk energy, the corresponding VEV requires an additional renormalization. As an example we can use the approach based on the

generalized zeta function approach. We plan to address these points in a separate publication.

## 6 The Casimir forces

The  $i$ th component of the force acting on the surface element  $dS$  of the brane at  $x^1 = a_j$  is given by  $-\langle T_l^i \rangle_{x^1=a_j+0} n_{(+j)}^l dS$  in the region  $x^1 \geq a_j + 0$  and by  $-\langle T_l^i \rangle_{x^1=a_j-0} n_{(-j)}^l dS$  in the region  $x^1 \leq a_j - 0$ , where  $n_{(\pm)j}^l = \pm \delta_1^l$ . For the resulting force we get

$$dF_{(j)}^i = \langle T_1^i \rangle_{x^1=a_j+0}^{x^1=a_j-0} dS. \quad (6.1)$$

Due to the nonzero off-diagonal stress  $\langle T_1^D \rangle$ , in addition to the normal component  $dF_{(j)}^1$ , this force has nonzero component parallel to the brane (shear force),  $dF_{(j)}^D$ . First we will consider the normal force.

### 6.1 Normal force

For the normal force acting on the brane at  $x^1 = a_j$  one has  $dF_{(j)}^1 = \langle T_1^1 \rangle_{z=a_j+0}^{z=a_j-0} dS$ . For  $\langle T_1^1 \rangle$  we have the decomposition (5.16) in the region between the branes and  $\langle T_1^1 \rangle = \langle T_1^1 \rangle_j$  in the remaining regions. The parts  $\langle T_1^1 \rangle_j$  are the same on the left and right-hand sides of the brane and they do not contribute to the net force. The nonzero contribution comes from the part  $\langle T_1^1 \rangle - \langle T_1^1 \rangle_j$  (given by the last term in (5.16)) in the region between the branes. Hence, for the vacuum effective pressure on the brane  $x^1 = a_j$ , given as  $P_j = -(\langle T_1^1 \rangle - \langle T_1^1 \rangle_j)_{x^1=a_j}$ , one gets

$$P_j = \frac{\alpha^{-1-D}}{2^{D+2\nu} \pi^{\frac{D-1}{2}}} \int_0^\infty dx x \frac{-2 + [2 + c_j(x/z) + 1/c_j(x/z)] \hat{B}_1}{c_1(x/z) c_2(x/z) e^{2ax/z} - 1} x^{D+2\nu} F_{\nu}^{\frac{D}{2}}(x). \quad (6.2)$$

The corresponding Casimir forces act on the sides  $x^1 = a_1 + 0$  and  $x^1 = a_2 - 0$ . They are attractive for  $P_j < 0$  and repulsive for  $P_j > 0$ . In the special cases of Dirichlet or Neumann boundary conditions the Casimir forces are obtained directly from (5.28) with  $i = 1$ :

$$P_j = -\frac{\alpha^{-1-D}}{2^{D+2\nu+2} \pi^{\frac{D}{2}}} \sum_{n=1}^{\infty} \left[ \partial_c^2 h_{\nu}^{\frac{D}{2}}(c) - 4(1-\delta_J) q_{\nu}^{(1)}(c) \right]_{c=na/z}. \quad (6.3)$$

For Dirichlet boundary condition on the brane  $x^1 = a_1$  and Neumann condition for  $x^1 = a_2$  the corresponding formula is obtained from (6.3) by the replacement (3.16).

The expression for the Casimir normal force in the Minkowskian limit directly follows from (5.26). The corresponding effective pressure is expressed as  $P_j^{(M)} = -\langle T_1^1 \rangle_{(M)}^{(0)}$ . Note that for the Minkowskian bulk the forces acting on separate plates coincide regardless of the values of the Robin coefficients. As seen from (6.2), in general this is not the case for the AdS geometry.

For small separations between the branes,  $a \ll z$ , the dominant contribution to the integral in (6.2) comes from the region with large  $x$  and we use the asymptotic (4.25) for the function  $F_{\nu}^{\mu}(x)$ . The leading term in the expansion of the force comes from the part with -2 in the numerator of the integrand in (6.2) and we get

$$P_j \approx -\frac{2(z/\alpha)^{D+1}}{(4\pi)^{\frac{D}{2}} \Gamma(\frac{D}{2})} \int_0^\infty d\lambda \frac{\lambda^D}{c_1(\lambda) c_2(\lambda) e^{2a\lambda} - 1}. \quad (6.4)$$

If additionally one has  $a \ll |\beta_l|$ ,  $l = 1, 2$ , we note that the integral in (6.4) is dominated by the contribution from the region  $\lambda \lesssim 1/a$  and in that region  $c_1(\lambda) c_2(\lambda) \approx 1$ . The estimate (6.4) is further simplified as

$$P_j \approx -\frac{D\zeta(D+1)}{(2\sqrt{\pi}\alpha a/z)^{D+1}} \Gamma\left(\frac{D+1}{2}\right), \quad (6.5)$$

where  $\zeta(x)$  is the Riemann zeta function. For Dirichlet boundary conditions on both the branes  $c_1(\lambda)c_2(\lambda) = 1$  and we get the same leading term. For Dirichlet boundary condition on one brane and non-Dirichlet condition on the other, with the modulus of the Robin coefficient much larger than  $a$ , we have  $c_1(\lambda)c_2(\lambda) \approx -1$ . In this case (6.4) is reduced to

$$P_j \approx \frac{D\zeta(D+1)}{(2\sqrt{\pi}\alpha a/z)^{D+1}} \left(1 - \frac{1}{2^D}\right) \Gamma\left(\frac{D+1}{2}\right). \quad (6.6)$$

The approximations (6.5) and (6.6) are obtained from the corresponding asymptotics for Robin plates in the Minkowski spacetime replacing the separation between the plates by the proper separation  $\alpha a/z$  in the AdS bulk. The asymptotics show that for small separations between the branes ( $a \ll z$  and  $a \ll |\beta_l|$  for non-Dirichlet boundary conditions) the Casimir normal forces are repulsive for Dirichlet boundary condition on one brane and non-Dirichlet condition on the other (formula (6.6)). In the remaining cases the forces are attractive. In the asymptotic region under consideration with the proper separation much smaller than the curvature radius, the effects of gravity on the Casimir forces are small and the results are similar to those for the Minkowski bulk.

We expect that the influence of the gravity will be essential for proper separations larger than the AdS curvature radius. In the limit  $a/z \gg 1$  the integral in (6.2) is dominated by the contribution from the region with small  $x$ . Expanding the function  $F_\nu^{D/2}(x)$  in (6.2) one finds

$$P_j \approx \frac{2\pi^{\frac{1-D}{2}} \alpha^{-1-D} (z/2)^{D+2\nu}}{\Gamma\left(\frac{D+1}{2} + \nu\right) \Gamma(1+\nu)} \int_0^\infty d\lambda \lambda^{D+2\nu-1} \frac{\nu B_\nu [2+c_j(\lambda) + 1/c_j(\lambda)] - \lambda^2 z^2}{c_1(\lambda)c_2(\lambda)e^{2a\lambda} - 1}, \quad (6.7)$$

where  $B_\nu$  is defined by (5.36). Under additional conditions  $a \gg |\beta_l|$ ,  $l = 1, 2$  (non-Neumann boundary conditions on both the branes), we further expand the integrand over the small ratio  $|\beta_l|/a$  with the result

$$P_j \approx -\frac{2(D+2\nu+1) \left(4\nu B_\nu \beta_j^2/z^2 + 1\right)}{\pi^{\frac{D}{2}} \Gamma(1+\nu) \alpha^{D+1} (2a/z)^{D+2\nu+2}} \zeta(D+2\nu+2) \Gamma\left(\frac{D}{2} + \nu + 1\right), \quad (6.8)$$

For  $a \gg |\beta_j|$  and for Neumann boundary condition on the second brane ( $c_{j'}(\lambda) = 1$ , as before,  $j' = 1$  for  $j = 2$  and  $j' = 2$  for  $j = 1$ ) from (6.7) we get

$$P_j \approx \frac{2(D+2\nu+1) \left(4\nu B_\nu \beta_j^2/z^2 + 1\right)}{\pi^{\frac{D}{2}} \Gamma(1+\nu) \alpha^{D+1} (2a/z)^{D+2\nu+2}} \times \left(1 - \frac{1}{2^{D+2\nu+1}}\right) \zeta(D+2\nu+2) \Gamma\left(\frac{D}{2} + \nu + 1\right). \quad (6.9)$$

The forces corresponding to (6.8) and (6.9) have opposite signs. As it has been already mentioned before, the coefficient  $B_\nu$  is negative for minimally and conformally coupled fields. Then, from (6.8) we see that, depending on the boundary conditions, the Casimir forces can be either attractive or repulsive at large distances. The sign of the forces is determined by the factor  $4\nu B_\nu \beta_j^2/z^2 + 1$ . This factor is positive near the horizon and is negative near the AdS boundary if  $B_\nu < 0$ . This shows that, for given values of the parameters, the vacuum pressure changes the sign as a function of  $z$ .

For Neumann boundary condition on the brane at  $x^1 = a_j$  and at large separations, to the leading order, we can ignore the term  $\lambda^2 z^2$  in (6.7). For non-Neumann boundary condition on the second brane, assuming  $a \gg |\beta_{j'}|$ , this gives

$$P_j \approx -\frac{4\nu B_\nu (1 - 2^{1-D-2\nu}) \zeta(D+2\nu)}{\pi^{\frac{D}{2}} \Gamma(1+\nu) \alpha^{D+1} (2a/z)^{D+2\nu}} \Gamma\left(\frac{D}{2} + \nu\right). \quad (6.10)$$

By taking into account that  $B_\nu < 0$  for minimal and conformal couplings, this result shows that for Neumann boundary condition on the brane  $x^1 = a_j$  and for non-Neumann condition on the second

brane the force is repulsive at large separations. For Neumann boundary condition on both the branes the leading term is expressed as

$$P_j \approx \frac{4\nu B_\nu \zeta(D+2\nu) \Gamma(D/2+\nu)}{\pi^{\frac{D}{2}} \Gamma(1+\nu) \alpha^{D+1} (2a/z)^{D+2\nu}}, \quad (6.11)$$

and the force is attractive for  $B_\nu < 0$ . The decay of the normal force at large proper separations between the branes is power-law for both massless and massive cases. In the Minkowski bulk and for massive fields the corresponding suppression is exponential. The leading term is found from (5.26),  $P_j^{(M)} \propto a^{-D/2} e^{-2ma}$ .

As seen from the analysis given above, for the brane with Neumann boundary condition the Casimir force on that brane decays at large separations like  $(z/a)^{D+2\nu}$  regardless the boundary condition on the second brane (except the special case with  $B_\nu = 0$ ). For non-Neumann boundary conditions on the brane at  $x^1 = a_j$  and for  $a \gg |\beta_j|$  the corresponding force behaves as  $(z/a)^{D+2\nu+2}$  and the suppression is stronger. As an example let us consider the case of Dirichlet boundary condition for  $x^1 = a_1$  and Neumann condition for  $x^1 = a_2$ . At large separations the Casimir pressure on the brane  $x^1 = a_1$  is given by (6.9) with  $j = 1$  and  $\beta_j = 0$ . It corresponds to a repulsive force. The leading term for the Casimir force on the brane  $x^1 = a_2$  is obtained from (6.10) with  $j = 2$ . The force is repulsive for  $B_\nu < 0$  and attractive for  $B_\nu > 0$ . This shows that, in principle, we can have a situation when the force has an attractive nature for one brane and repulsive nature for another.

In Figure 4 we have displayed the normal Casimir force versus the proper separation between the branes, in units of the AdS curvature radius, for  $D = 4$  minimally coupled scalar field. The same boundary conditions are imposed on the branes. The numbers near the curves are the values for  $\beta_1/z = \beta_2/z$ . The dashed and dotted curves correspond to Dirichlet and Neumann boundary conditions, respectively. The graphs are plotted for  $m\alpha = 0.5$ . The presented graphs demonstrate the feature already seen from asymptotic analysis: the forces attractive at small separations may become repulsive for larger distances.

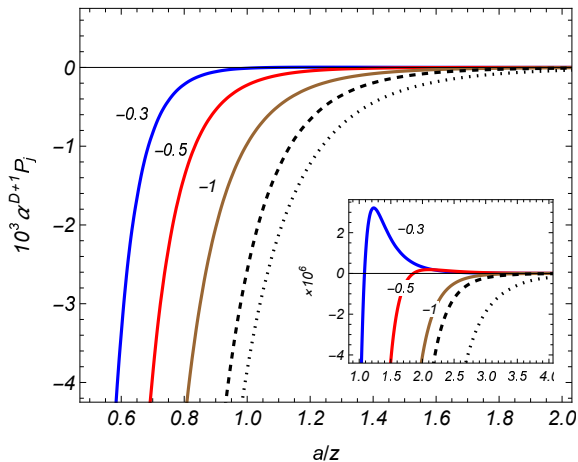


Figure 4: The Casimir normal force for  $D = 4$  minimally coupled field with  $m\alpha = 0.5$  as a function of the interbrane separation. The graphs are plotted for Dirichlet and Neumann boundary conditions (dashed and dotted curves), and for Robin boundary conditions with the coefficients  $\beta_1/z = \beta_2/z$  given near the corresponding graphs.

Figure 5 presents the dependence of the Casimir normal force acting on the brane at  $x^1 = a_1$ , given by (6.2) with  $j = 1$ , on the coefficient in the Robin boundary condition on that brane. The left and right panels correspond to  $D = 4$  conformally and minimally coupled fields with  $m\alpha = 0.5$ . For the proper separation between the branes we have taken  $a/z = 1$ . The graphs are plotted for different boundary

conditions on the second brane: Dirichlet and Neumann conditions (Dir and Neu, respectively), Robin boundary conditions with  $\beta_2/z$  given near the curves. The dashed lines correspond to Dirichlet and Neumann conditions on both the branes (DD and NN), Dirichlet (Neumann) condition at  $x^1 = a_1$  and Neumann (Dirichlet) condition at  $x^1 = a_2$ , indicated as DN (ND). The graphs show that depending on the coefficient in the Robin boundary conditions the force can be either attractive or repulsive.

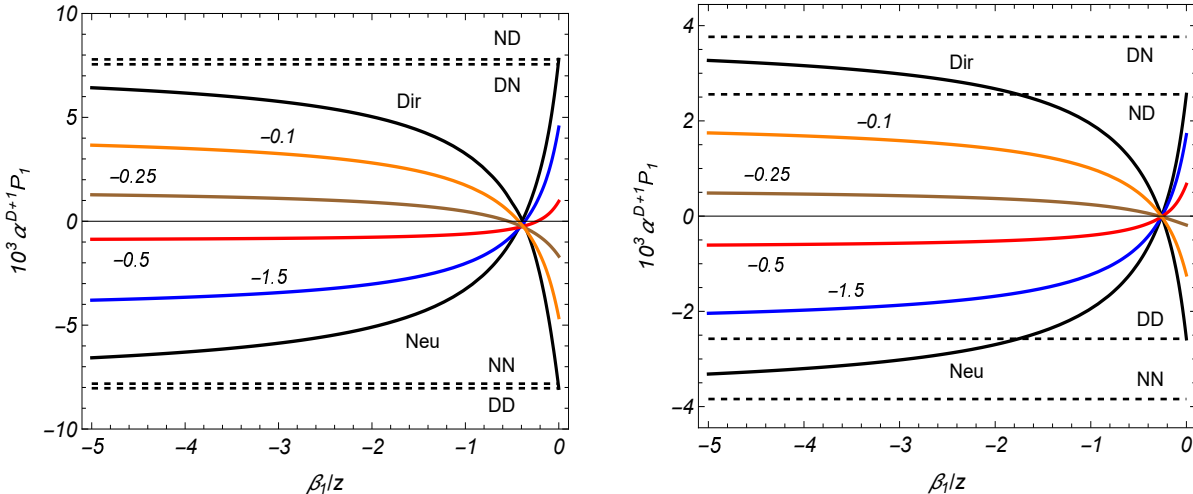


Figure 5: The Casimir normal force per unit surface of the brane  $x^1 = a_1$  as a function of the Robin coefficient in the boundary condition on that brane for  $D = 4$  conformally (left panel) and minimally (right panel) coupled fields. The graphs are plotted for  $m\alpha = 0.5$ ,  $a/z = 1$ , and for different boundary conditions on the second brane (see the text).

## 6.2 Shear force

As it has been emphasized above, in the problem at hand in addition to the normal Casimir force one has a nonzero shear force along the  $z$ -direction,  $dF_{(j)}^D = f_{(j)} dS$ , where  $f_{(j)}$  is the shear force per unit surface of the plate at  $z = z_j$ . The latter is given by  $f_{(j)} = \langle T_1^D \rangle_j|_{x^1=a_j-0}^{x^1=a_j+0}$ . In accordance with the decomposition (5.17), the shear force contains two contributions. The first part comes from the term  $\langle T_1^D \rangle_j$  and corresponds to the force acting on the brane at  $x^1 = a_j$  when the second brane is absent. We will call this part the self-acting shear force and will denote by  $f_j^{(s)}$ . Those forces acting on the sides  $x^1 = a_j - 0$  and  $x^1 = a_j + 0$  coincide and we get

$$f_j^{(s)} = \langle T_1^D \rangle_j|_{x^1=a_j-0}^{x^1=a_j+0} = \frac{4\alpha^{-1-D}}{2^{D+2\nu}\pi^{\frac{D-1}{2}}} \int_0^\infty dx \frac{1}{c_j(x/z)} \left[ \left( \xi - \frac{1}{4} \right) x \partial_x + \xi \right] x^{D+2\nu} F_{\nu^2}^{\frac{D}{2}}(x). \quad (6.12)$$

By using the asymptotic (4.25), we see that for nonconformally coupled fields and for large  $x$  the integrand in (6.12) behaves like  $x^{D-1}$  and the integral is divergent in the upper limit. For the conformal coupling the next to the leading term should be kept and the integral is still divergent. Of course, the divergence comes from the surface divergences in the single brane contributions to the VEVs. The renormalization of the divergence in the self-action shear force can be considered in the same line as that for the total and surface Casimir energies and will be discussed elsewhere. Here we will be focused on the contribution to the shear force that is induced by the second brane. This part acts on the sides  $x^1 = a_1 + 0$  and  $x^1 = a_2 - 0$  and is determined from the last term in (5.17). Denoting it by

$f_j^{(\text{int})}$ , we get

$$f_j^{(\text{int})} = -\frac{2\alpha^{-1-D}}{2^{D+2\nu}\pi^{\frac{D-1}{2}}} \int_0^\infty dx \frac{c_j(x/z) - 1/c_j(x/z)}{c_1(x/z)c_2(x/z)e^{2ax/z} - 1} \left[ \left( \xi - \frac{1}{4} \right) x \partial_x + \xi \right] x^{D+2\nu} F_\nu^{\frac{D}{2}}(x). \quad (6.13)$$

This part acting on the brane at  $x^1 = a_j$  vanishes for Dirichlet and Neumann boundary conditions on that brane regardless of boundary conditions on the second brane. The shear force is directed toward the horizon for  $f_j^{(\text{int})} > 0$  and toward the AdS boundary for  $f_j^{(\text{int})} < 0$ .

The asymptotic behavior of the shear force is found in a way similar to that for the normal force. At small proper separations compared with the curvature radius,  $a/z \ll 1$ , one gets

$$f_j^{(\text{int})} \approx -\frac{2D(\xi - \xi_D)z^D}{2^D\pi^{\frac{D}{2}}\Gamma\left(\frac{D}{2}\right)\alpha^{D+1}} \int_0^\infty d\lambda \lambda^{D-1} \frac{c_j(\lambda) - 1/c_j(\lambda)}{c_1(\lambda)c_2(\lambda)e^{2a\lambda} - 1}. \quad (6.14)$$

For a conformally coupled field the leading term vanishes and the next term in the expansion should be kept. If additionally  $|\beta_l| \gg a$ ,  $l = 1, 2$  (the condition with  $l = j'$  is required only for non-Dirichlet boundary conditions on the brane at  $x^1 = a_{j'}$ ), the further expansion gives

$$f_j^{(\text{int})} \approx \frac{4D(\xi - \xi_D)\zeta(D-1)}{\pi^{\frac{D+1}{2}}\alpha^{D+1}(2a/z)^D b_j} \Gamma\left(\frac{D-1}{2}\right) (2^{2-D} - 1)^{\delta_{0b_{j'}}}, \quad (6.15)$$

where the last factor is present only for Dirichlet boundary condition at  $x^1 = a_{j'}$ . Note that under the specified conditions one has  $|b_j| \gg 1$ . As seen, at small separations, the shear component of the force has opposite signs for Dirichlet and non-Dirichlet boundary conditions on the second brane. For a minimally coupled field with  $b_j < 0$  and for small separations the shear force acting on the brane at  $x^1 = a_j$  is directed toward the AdS horizon for non-Dirichlet boundary conditions on the second brane and toward the AdS boundary for Dirichlet condition.

At large proper separations,  $a/z \gg 1$ , the interaction force is approximated by

$$f_j^{(\text{int})} \approx -\frac{2\pi^{\frac{1-D}{2}}B_\nu\alpha^{-1-D}(z/a)^{D+2\nu+1}}{2^{D+2\nu}\Gamma(\nu+1)\Gamma\left(\frac{D+1}{2}+\nu\right)} \int_0^\infty dx \frac{c_j(x/a) - 1/c_j(x/a)}{c_1(x/a)c_2(x/a)e^{2x} - 1} x^{D+2\nu}. \quad (6.16)$$

This estimate is further simplified under the condition  $|\beta_l| \ll a$ ,  $l = 1, 2$  (the condition for  $l = j'$  is required only for non-Neumann boundary conditions at  $x^1 = a_{j'}$ ):

$$f_j^{(\text{int})} \approx -\frac{4b_j B_\nu (D+2\nu+1)\zeta(D+2\nu+2)}{\pi^{\frac{D}{2}}\Gamma(\nu+1)\alpha^{D+1}(2a/z)^{D+2\nu+1}} \Gamma\left(\frac{D}{2}+\nu+1\right) \left(\frac{1}{2^{D+2\nu+1}} - 1\right)^{\delta_{\infty b_{j'}}}, \quad (6.17)$$

where  $B_\nu$  is defined by (5.36) and  $|b_j| \ll 1$ . The force (6.17) has opposite signs for Neumann and non-Neumann boundary conditions on the brane  $x^1 = a_{j'}$ . For conformally and minimally coupled fields one has  $B_\nu < 0$ . In those cases, for  $b_j < 0$  and at large separations between the branes the shear force acting on the brane  $x^1 = a_j$  is directed toward the AdS horizon for Neumann boundary condition on the second brane and toward the AdS boundary for non-Neumann conditions.

The interaction part of the shear force acting on the brane  $x^1 = a_1$  versus the distance between the branes is depicted in Figure 6 for  $D = 4$  conformally and minimally coupled field (left and right panels, respectively). The graphs are plotted for  $m\alpha = 0.5$  and for different values of the ratio  $\beta_1/z = \beta_2/z$  (the numbers near the curves). In both cases the shear force is directed toward the horizon at small separations between the branes and toward the AdS boundary at large separations. For a minimally coupled field this is in agreement with the asymptotic analysis presented above.

The interaction part of the shear force per unit surface of the brane  $x^1 = a_1$  is plotted in Figure 7 as a function of the ratio  $\beta_1/z$  for different boundary conditions on the second brane (Dirichlet, Neumann and Robin conditions with the values for  $\beta_2/z$  presented near the curves). The left and right panels correspond to conformally and minimally coupled fields in (4+1)-dimensional AdS spacetime. The graphs are plotted for  $m\alpha = 0.5$  and  $a/z = 1$ .



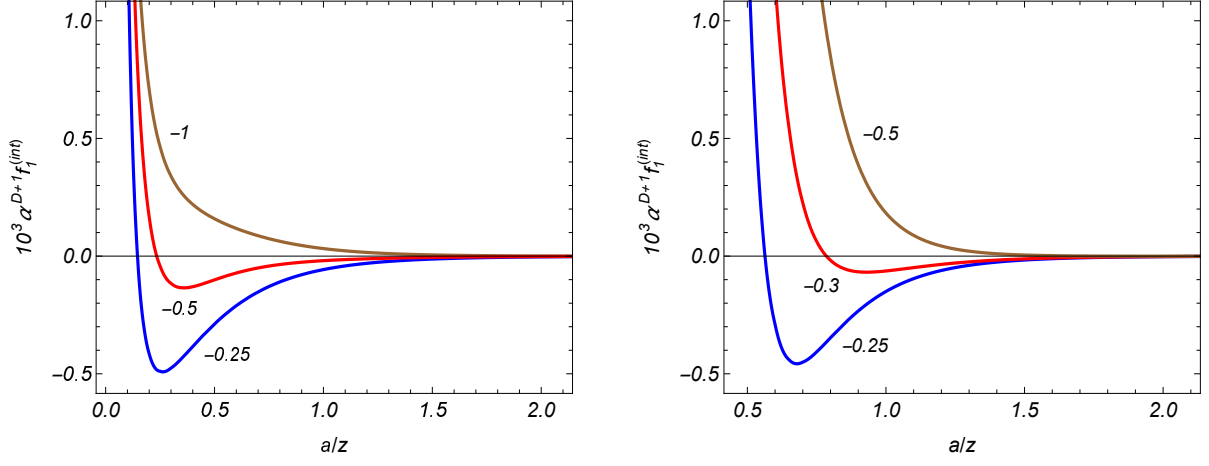


Figure 6: The interaction contribution to the shear force per unit surface of the brane  $x^1 = a_1$  versus the interbrane separation for different values of  $\beta_1/z = \beta_2/z$  (the numbers given near the curves). The graphs are plotted for  $D = 4$  conformally (left panel) and minimally (right panel) coupled fields with  $m\alpha = 0.5$ .

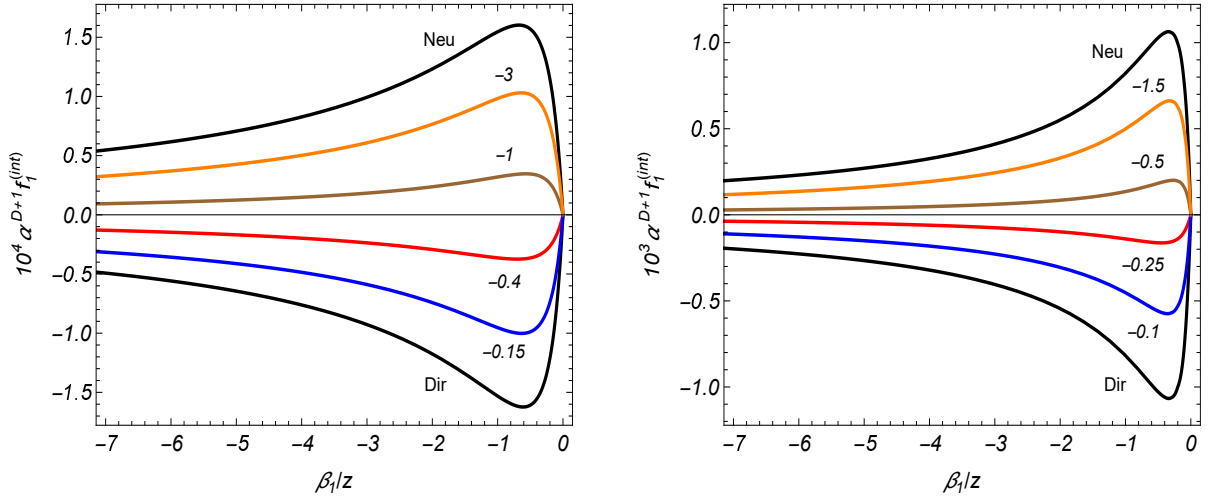


Figure 7: The interaction shear force acting on the brane  $x^1 = a_1$  versus the corresponding Robin coefficient for  $D = 4$  conformally (left panel) and minimally (right panel) coupled fields. The numbers near the curves are the values of the ratio  $\beta_2/z$  and the graphs are plotted for  $m\alpha = 0.5$ ,  $a/z = 1$ .

## 7 Conclusion

In this paper we have investigated the influence of two parallel branes, orthogonal to the AdS boundary, on the local properties of the scalar vacuum in background of  $(D + 1)$ -dimensional AdS spacetime. Robin boundary conditions are imposed, in general, with different coefficients on separate branes. We consider a free field theory and the properties of the vacuum are completely determined by the two-point functions. As a two-point function, the positive frequency Wightman function is chosen. The local VEVs are obtained in the coincidence limit of the arguments of that function and its derivatives. For the evaluation of the Wightman function the direct summation over the complete set of scalar modes is used. In the region between the branes the mode functions are given by (2.6) with the function  $\alpha_j(\lambda)$  defined as (2.9). The eigenvalues of the quantum number  $\lambda$  are discretized by the boundary conditions and they are expressed in terms of the roots of equation (2.10). The geometry of the subspace  $y = \text{const}$ , parallel to the AdS boundary, is Minkowskian and the eigenvalue equation coincides with that in the Casimir problem for two Robin plates in flat spacetime. For general Robin boundary conditions the eigenvalues of  $\lambda$  are given implicitly and for the summation of the corresponding series in the mode sum of the Wightman function we have employed the Abel-Plana-type formula (A.1). This has two advantages: (i) an integral representation is provided for which the explicit knowledge of the eigenvalues is not required and (ii) the parts corresponding to the brane-free and single brane geometries are explicitly extracted. In particular, on the basis of (ii), the renormalization of local VEVs for points outside the branes is reduced to the one in the brane-free problem.

As a local characteristic of the vacuum state we have considered the mean field squared. Based on the Wightman function decomposition, the VEV is presented in two equivalent forms, (4.5) and (4.6). In the second one the contribution corresponding to the problem with a single brane is separated. For special cases of Dirichlet and Neumann boundary conditions the VEVs are further simplified to (4.14). An alternative representation for those cases is given by (4.18). For a conformally coupled massless scalar field the problem under consideration is conformally related to the problem with parallel Robin plates in the Minkowski spacetime orthogonally intersected by a Dirichlet plate, the latter being the conformal image of the AdS boundary. The Dirichlet boundary condition on the conformal image is related to the condition for the field modes (2.6) imposed on the AdS boundary. In the Minkowskian limit we recover the result for a massive scalar field in the geometry of two parallel plates, previously considered in [21] and [22] for massless and massive fields, respectively. For points near the branes and not too close to the AdS boundary the dominant contribution to the VEV comes from quantum fluctuations with wavelengths smaller than the curvature radius and the influence of the gravity is weak. The leading term in the expansion over the distance from the brane coincides with that for a plate in the Minkowski bulk with the distance from the plate replaced by the proper distance in the AdS bulk. The brane-induced contribution vanishes on the AdS boundary. For points not too close to the branes the corresponding asymptotic is given by (4.24). In the opposite near-horizon limit, for fixed value of the coordinate distance  $a$ , the proper separation between the branes is small compared to the curvature radius and the brane-induced VEV is well approximated by the Minkowskian expression (see (4.26)). Depending on the boundary conditions, the mean field squared, as a function of the distance from the brane, may change the sign.

The vacuum energy density and stresses in the region between the branes have been discussed in Section 5. The diagonal components of the vacuum energy-momentum tensor are given by the formula (5.7). The only nonzero off-diagonal component corresponds to the stress  $\langle T_D^1 \rangle$ , expressed as (5.10). The generation of this component is a pure brane-induced effect and gives rise to a shear force acting on the branes. As expected, the brane-induced contribution obeys the trace relation (5.11) and the covariant conservation equation. Single brane contributions in the components of the vacuum energy-momentum tensor are explicitly separated in the representations (5.16) and (5.17). In the Minkowskian limit we recover the results of Refs. [21] and [22] for massless and massive scalar fields. In the special

case of a conformally coupled massless field the brane-induced part has a conformal connection with the corresponding vacuum energy-momentum tensor for two parallel plates with Robin boundary conditions intersected by the third plate with Dirichlet boundary condition. The respective VEVs are given by (5.20) and (5.24). For special cases of Dirichlet and Neumann boundary conditions equivalent representations are given by formulae (5.28) and (5.32). Near the branes and near the horizon, for fixed value of the separation  $a$ , the effects of the gravity on the brane-induced VEVs of the components  $\langle T_i^i \rangle$  with  $i \neq 1$  are weak and the leading terms in the corresponding expansions coincide with those for the Minkowski bulk. The brane-induced contributions in the diagonal components vanish on the AdS boundary like  $z^{D+2\nu}$ . The decay for the off-diagonal component is stronger, as  $z^{D+2\nu+1}$ . The numerical investigation for the distribution of the vacuum energy density is presented for the case when the boundary conditions imposed on separate branes are the same. The brane-induced vacuum energy density in the region between the branes is negative for Dirichlet boundary conditions and positive for Neumann conditions. For Robin conditions there is a critical value of the coefficient  $\beta_j = \beta_j^{(c)} < 0$  that separates two qualitatively different distributions. For  $\beta_j < \beta_j^{(c)}$  the behavior of the energy density is of Neuman-type: the energy density is positive everywhere in the region between the branes. In the range  $\beta_j^{(c)} < \beta_j < 0$  the energy density is positive near the branes and negative near the center with respect to the brane locations. This type of behavior is depicted in Figure 3.

The Casimir forces acting on the branes have two components. The first one corresponds to the normal force which is considered in the literature for different bulk and boundary geometries. Interpreted in terms of the vacuum pressure on the brane at  $x^1 = a_j$ , it is given by the expression (6.2) or by an alternative representation (6.3) for Dirichlet and Neumann boundary conditions. Unlike the problem in the Minkowskian bulk, the forces for Dirichlet and Neumann boundary conditions are different. Another difference is that the forces acting on separate branes differ if the coefficients in the Robin boundary conditions on them are different. Depending on the boundary conditions and on the separation between the branes the normal forces can be either attractive or repulsive. At small separations the effects of background curvature are weak and the force is well approximated by the corresponding result for the Minkowski bulk. They are repulsive for Dirichlet boundary condition on one brane and non-Dirichlet condition on the other and attractive in the remaining cases. The influence of gravity is essential for proper separations larger than the AdS curvature radius. The decay of forces at large separations is power-law for both cases of massless and massive fields. For massive fields this results is in contrast to the exponential decay in the Minkowski bulk. The Casimir normal force acting on the brane decays at large separations like  $(z/a)^{D+2\nu}$  for Neumann boundary condition on that brane and behaves as  $(z/a)^{D+2\nu+2}$  for non-Neumann boundary conditions with  $|\beta_j| \ll a$ . The large-distance asymptotic behavior of the vacuum effective pressure on the brane at  $x^1 = a_j$  is given by (6.8) and (6.9) for non-Neumann boundary conditions on that brane and by (6.10) and (6.11) for Neumann condition. The sign of the force at large separations depend on the parameter  $B_\nu$ , defined by (5.36). For given values of the parameters, the vacuum pressure may also change its sign as a function of  $z$ . This means that the forces acting on different parts of the brane may differ by sign.

A qualitatively different feature of the problem in the AdS bulk is the presence of the vacuum shear force on the branes. The corresponding part induced by the second brane is expressed as (6.13). It vanishes for the brane with Dirichlet or Neumann boundary conditions regardless of the condition on the second brane. Depending on the coefficients in the boundary conditions, on the separation between the branes and also on the distance from the AdS boundary, the shear component of the force can be either positive or negative. At small separations, the leading term in the expansion of the shear force is given by (6.15). In particular, for a minimally coupled field with negative value of the Robin coefficient  $\beta_j$  the shear force on the brane  $x^1 = a_j$  is directed toward the AdS horizon for non-Dirichlet boundary conditions on the second brane and toward the AdS boundary for Dirichlet condition. At large separations the asymptotic for the interaction part of the shear force is given by (6.17). For minimally and conformally coupled fields and for  $\beta_j < 0$ , at large separations the force

$f_j^{(\text{int})}$  is directed toward the AdS horizon for Neumann boundary condition on the second brane and toward the AdS boundary for non-Neumann conditions.

## Acknowledgments

A.A.S. was supported by the grants No. 20RF-059 and No. 21AG-1C047 of the Science Committee of the Ministry of Education, Science, Culture and Sport RA. V.Kh.K. was supported by the grant No. 21AG-1C069 of the Science Committee of the Ministry of Education, Science, Culture and Sport RA. A.A.S. gratefully acknowledges the hospitality of the INFN, Laboratori Nazionali di Frascati (Frascati, Italy), where a part of this work was done.

## A Integral representation for the series over eigenvalues

In this section we provide an integral representation for the series  $S(b, \Delta t, x^1, x'^1)$ , given by (3.4). The transformation will be based on the summation formula [21]

$$\sum_{n=1}^{\infty} \frac{f(u_n)}{N_n} = \frac{1}{\pi} \int_0^{\infty} du f(u) + \frac{i}{\pi} \int_0^{\infty} du \frac{f(e^{\pi i/2} u) - f(e^{-\pi i/2} u)}{\tilde{c}_1(u) \tilde{c}_2(u) e^{2u} - 1} - \frac{f(0)/2}{1 - b_2 - b_1} - \frac{\theta(b_j)}{2b_j} \left[ h_1(e^{\pi i/2}/b_j) + h_1(e^{-\pi i/2}/b_j) \right], \quad (\text{A.1})$$

where  $\theta(x)$  is the Heaviside step function,  $\tilde{c}_j(u) = (b_j u - 1)/(b_j u + 1)$  and  $h(u) = (b_j^2 u^2 + 1)f(u)$ . In (A.1) it is assumed that the function  $f(u)$  is analytic in the right half-plane  $\text{Re } u > 0$ . For the series in (3.2) the function  $f(u)$  is given by the expression

$$f(u) = \frac{e^{-i\sqrt{u^2/a^2 + b^2}\Delta t}}{\sqrt{u^2/a^2 + b^2}} \left[ 2 \cos\left(\frac{u}{a}\Delta x^1\right) + \sum_{l=\pm 1} \left( e^{i|x^1 + x'^1 - 2a_j|u/a} \frac{iub_j - 1}{iub_j + 1} \right)^l \right], \quad (\text{A.2})$$

with  $f(0) = 0$ . By taking into account that for  $x > 0$  one has

$$\sqrt{(e^{\pm\pi i/2} x)^2 + b^2} = \begin{cases} \sqrt{b^2 - x^2}, & x < b \\ e^{\pm\pi i/2} \sqrt{x^2 - b^2}, & x > b \end{cases}, \quad (\text{A.3})$$

and introducing a new integration variable  $\lambda = u/a$ , the function (3.4) is presented as

$$S(b, \Delta t, x^1, x'^1) = \frac{a}{2} S_0(b, \Delta t, x^1_{-}) + \frac{a}{4} S_j(b, \Delta t, x^1_{+}) + a \frac{\pi \theta(\beta_j)}{2\beta_j} e^{-|x^1_{+} - 2a_j|/\beta_j} \sum_{l=\pm 1} \frac{e^{-i\sqrt{(li/\beta_j)^2 + b^2}\Delta t}}{\sqrt{(li/\beta_j)^2 + b^2}} + \frac{a}{2} \int_b^{\infty} d\lambda \frac{2 \cosh(\lambda x^1_{-}) + \sum_{l=\pm 1} \left[ e^{i|x^1_{+} - 2a_j|\lambda} c_j(\lambda a) \right]^l}{[c_1(\lambda a) c_2(\lambda a) e^{2a\lambda} - 1] \sqrt{\lambda^2 - b^2}} \cosh\left(\sqrt{\lambda^2 - b^2}\Delta t\right), \quad (\text{A.4})$$

where  $x^1_{\pm} = x^1 \pm x'^1$  and

$$S_0(b, \Delta t, x^1_{-}) = \int_0^{\infty} d\lambda \frac{e^{-i\sqrt{\lambda^2 + b^2}\Delta t}}{\sqrt{\lambda^2 + b^2}} \cos(\lambda x^1_{-}),$$

$$S_j(b, \Delta t, x^1_{+}) = \int_0^{\infty} d\lambda \frac{e^{-i\sqrt{\lambda^2 + b^2}\Delta t}}{\sqrt{\lambda^2 + b^2}} \sum_{l=\pm 1} \left( e^{i|x^1_{+} - 2a_j|\lambda} \frac{i\lambda\beta_j - 1}{i\lambda\beta_j + 1} \right)^l. \quad (\text{A.5})$$

For the further transformation of the function  $S_j(b, \Delta t, x^1_{+})$  we rotate the integration contour by the angle  $\pi/2$  for the  $l = 1$  term and by the angle  $-\pi/2$  for the term with  $l = -1$ . This choice for the

integration contours is dictated by the behavior of the integrands in the upper and lower half-planes of the complex variable  $\lambda$ . The poles  $\lambda = \pm i/\beta_j$  for  $\beta_j > 0$  are excluded by semicircles in the right half-plane  $\text{Re } \lambda \geq 0$  with small radius. Again, by using (A.3), this gives

$$S_j(b, \Delta t, x_+^1) = 2 \int_b^\infty d\lambda \frac{\cosh\left(\sqrt{\lambda^2 - b^2} \Delta t\right) e^{-\lambda|x_+^1 - 2a_j|}}{\sqrt{\lambda^2 - b^2} c_j(\lambda a)} - \frac{2\pi}{\beta_j} \theta(\beta_j) \sum_{l=\pm 1} \frac{e^{-i\sqrt{(i/\beta_j)^2 + b^2} \Delta t}}{\sqrt{(i/\beta_j)^2 + b^2}} e^{-|x_+^1 - 2a_j|/\beta_j}. \quad (\text{A.6})$$

Substituting this in (A.4) we see that the terms with the Heaviside step function are cancelled out and the function (3.4) is expressed as

$$S(b, \Delta t, x^1, x'^1) = \frac{a}{2} S_0(b, \Delta t, \Delta x^1) + \frac{a}{2} \int_b^\infty d\lambda \frac{\cosh\left(\sqrt{\lambda^2 - b^2} \Delta t\right) e^{-\lambda|x_+^1 - 2a_j|}}{\sqrt{\lambda^2 - b^2} c_j(\lambda a)} + \frac{a}{2} \int_b^\infty d\lambda \frac{2 \cosh(\lambda x_-^1) + \sum_{l=\pm 1} \left[ e^{|\lambda x_+^1 - 2a_j|} c_j(\lambda a) \right]^l}{[c_1(\lambda a) c_2(\lambda a) e^{2a\lambda} - 1] \sqrt{\lambda^2 - b^2}} \cosh\left(\sqrt{\lambda^2 - b^2} \Delta t\right). \quad (\text{A.7})$$

Another representation, symmetric with respect to the branes, is obtained from (A.7) combining the integrals:

$$S(b, \Delta t, x^1, x'^1) = \frac{a}{2} S_0(b, \Delta t, \Delta x^1) + \frac{a}{2} \int_b^\infty d\lambda \frac{\cosh\left(\sqrt{\lambda^2 - b^2} \Delta t\right)}{\sqrt{\lambda^2 - b^2}} \times \frac{2 \cosh(\lambda x_-^1) + \sum_{j=1,2} e^{|\lambda x_+^1 - 2a_j|} c_j(\lambda a)}{c_1(\lambda a) c_2(\lambda a) e^{2a\lambda} - 1}. \quad (\text{A.8})$$

Note that in the limit  $(-1)^{j'} a_{j'} \rightarrow +\infty$ , with  $j' = 1$  for  $j = 2$  and  $j' = 2$  for  $j = 1$ , the last term in (A.7) goes to zero and the first two terms in the right-hand side determine the contribution to the Wightman function in the geometry of a single brane at  $x^1 = a_j$ .

## References

- [1] V.M. Mostepanenko and N.N. Trunov, *The Casimir Effect and Its Applications* (Clarendon, Oxford, 1997); K.A. Milton, *The Casimir Effect: Physical Manifestation of Zero-Point Energy* (World Scientific, Singapore, 2002); V.A. Parsegian, *Van der Waals Forces: A Handbook for Biologists, Chemists, Engineers, and Physicists* (Cambridge University Press, Cambridge, England, 2005); M. Bordag, G.L. Klimchitskaya, U. Mohideen, and V.M. Mostepanenko, *Advances in the Casimir Effect* (Oxford University Press, New York, 2009); *Casimir Physics*, edited by D. Dalvit, P. Milonni, D. Roberts, and F. da Rosa, Lecture Notes in Physics Vol. 834 (Springer-Verlag, Berlin, 2011).
- [2] O. Aharony, S. S. Gubser, J. Maldacena, H. Ooguri, and Y. Oz, Phys. Rep. **323**, 183 (2000); M. Natsuume, *AdS/CFT Duality User Guide*, Lecture Notes in Physics Vol. 903 (Springer, Tokyo, Japan, 2015).
- [3] R. Maartens and K. Koyama, Living Rev. Relativity **13**, 5 (2010).
- [4] L. Randall and R. Sundrum, Phys. Rev. Lett. **83**, 3370 (1999); L. Randall and R. Sundrum, Phys. Rev. Lett. **83**, 4690 (1999).

- [5] M. Fabinger and P. Horava, Nucl. Phys. B **580**, 243 (2000); S. Nojiri, S. Odintsov, and S. Zerbini, Phys. Rev. D **62**, 064006 (2000); S. Nojiri, O. Obregon, and S. Odintsov, Phys. Rev. D **62**, 104003 (2000); D. J. Toms, Phys. Lett. B **484**, 149 (2000); W. D. Goldberger and I. Z. Rothstein, Phys. Lett. B **491**, 339 (2000); J. Garriga, O. Pujolàs, and T. Tanaka, Nucl. Phys. B **605**, 192 (2001); E. Elizalde, S. Nojiri, S. D. Odintsov, and S. Ogushi, Phys. Rev. D **67**, 063515 (2003); A. Flachi and O. Pujolàs, Phys. Rev. D **68**, 025023 (2003); A. Flachi, J. Garriga, O. Pujolàs, and T. Tanaka, J. High Energy Phys. 08 (2003) 053; R. Durrer and M. Ruser, Phys. Rev. Lett. **99**, 071601 (2007); M. Ruser and R. Durrer, Phys. Rev. D **76**, 104014 (2007); R. Linares, H.A. Morales-Técotl, and O. Pedraza, Phys. Rev. D **77**, 066012 (2008); M. Frank, N. Saad, and I. Turan, Phys. Rev. D **78**, 055014 (2008); A. Flachi and T. Tanaka, Phys. Rev. D **80**, 124022 (2009); L. P. Teo, Phys. Lett. B **682**, 259 (2009).
- [6] A. Flachi and D. J. Toms, Nucl. Phys. B **610**, 144 (2001).
- [7] A. Flachi, I. G. Moss, and D. J. Toms, Phys. Lett. B **518**, 153 (2001); A. Flachi, I. G. Moss, and D. J. Toms, Phys. Rev. D **64**, 105029 (2001); K. Uzawa, Prog. Theor. Phys. **110**, 457 (2003).
- [8] J. Garriga and A. Pomarol, Phys. Lett. B **560**, 91 (2003); L. P. Teo, J. High Energy Phys. 10 (2010) 019.
- [9] A. A. Saharian and M. R. Setare, Phys. Lett. B **552**, 119 (2003); R. A. Knapman and D. J. Toms, Phys. Rev. D **69**, 044023 (2004); A. A. Saharian, Phys. Rev. D **73**, 044012 (2006); A. A. Saharian, Phys. Rev. D **73**, 064019 (2006); S.-H. Shao, P. Chen, and J.-A. Gu, Phys. Rev. D **81**, 084036 (2010); E. Elizalde, S. D. Odintsov, and A. A. Saharian, Phys. Rev. D **87**, 084003 (2013); A. S. Kotanjyan and A. A. Saharian, Phys. At. Nucl. **80**, 562 (2017); A. S. Kotanjyan, A. A. Saharian, and A. A. Saharyan, Galaxies **5**, 102 (2017); A. A. Saharian, A. S. Kotanjyan, and H. G. Sargsyan, Phys. Rev. D **102**, 105014 (2020).
- [10] A. A. Saharian, Nucl. Phys. **B712**, 196 (2005).
- [11] A. A. Saharian and A. L. Mkhitarian, J. High Energy Phys. 08 (2007) 063.
- [12] S. Bellucci, W. Oliveira dos Santos, E. R. Bezerra de Mello, and A. A. Saharian, J. High Energy Phys. 05 (2022) 021; S. Bellucci, W. Oliveira dos Santos, E. R. Bezerra de Mello, and A. A. Saharian, J. Cosmol. Astropart. Phys. 01 (2022) 010.
- [13] S. Bellucci, A. A. Saharian, and V. Vardanyan, Phys. Rev. D **96**, 065025 (2017); S. Bellucci, A. A. Saharian, and V. Vardanyan, J. High Energy Phys. 11 (2015) 092; S. Bellucci, A. A. Saharian, and V. Vardanyan, Phys. Rev. D **93**, 084011 (2016); S. Bellucci, A. A. Saharian, D. H. Simonyan, and V. Vardanyan, Phys. Rev. D **98**, 085020 (2018); S. Bellucci, A. A. Saharian, H. G. Sargsyan, and V. V. Vardanyan, Phys. Rev. D **101**, 045020 (2020).
- [14] G. Cuomo, M. Mezei, and A. Raviv-Moshe, J. High Energy Phys. 10 (2021) 143.
- [15] T. Takayanagi, Phys. Rev. Lett. **107**, 101602 (2011); M. Fujita, T. Takayanagi, and E. Tonni, J. High Energy Phys. 11 (2011) 043.
- [16] S. Ryu and T. Takayanagi, Phys. Rev. Lett. **96**, 181602 (2006); S. Ryu and T. Takayanagi, J. High Energy Phys. 08 (2006) 045.
- [17] T. Nishioka, S. Ryu, and T. Takayanagi, J. Phys. A: Math. Theor. **42**, 504008 (2009).
- [18] B. Chen, B. Czech, and Zi-Zhi Wang, Rep. Prog. Phys. **85**, 046001 (2022).
- [19] E. R. Bezerra de Mello, A. A. Saharian, and M. R. Setare, Phys. Rev. D **92**, 104005, (2015).

- [20] P. Breitenlohner and D. Z. Freedman, *Ann. Phys. (N.Y.)* **144**, 249 (1982).
- [21] A. Romeo and A. A. Saharian, *J. Phys. A: Math. Gen.* **35**, 1297 (2002).
- [22] A. A. Saharian, *The Generalized Abel-Plana Formula with Applications to Bessel Functions and Casimir Effect* (Yerevan State University, Yerevan, 2008); The Abdus Salam International Centre for Theoretical Physics, Report No. ICTP/2007/082; arXiv:0708.1187.
- [23] I. S. Gradshteyn and I. M. Ryzhik, *Table of Integrals, Series, and Products* (Academic Press, New York, 2007).
- [24] A. P. Prudnikov, Yu. A. Brychkov, and O. I. Marichev, *Integrals and Series* (Gordon and Breach, New York, 1986), Vol. 2.
- [25] N. D. Birrell and P. C. W. Davies, *Quantum Fields in Curved Space* (Cambridge University Press, Cambridge, England, 1982).
- [26] A. Ishibashi and R.M. Wald, *Class. Quantum Gravity* **21**, 2981 (2004); C. Dappiaggi and H. R. C. Ferreira, *Phys. Rev. D* **94**, 125016 (2016); C. Dappiaggi, H. R. C. Ferreira, and A. Marta, *Phys. Rev. D* **98**, 025005 (2018); T. Morley, P. Taylor, and E. Winstanley, *Class. Quantum Grav.* **38**, 035009 (2021).
- [27] A. P. Prudnikov, Yu. A. Brychkov, and O. I. Marichev, *Integrals and Series* (Gordon and Breach, New York, 1990), Vol. 3.
- [28] *Handbook of Mathematical Functions*, edited by M. Abramowitz and I. A. Stegun (Dover, New York, 1972).
- [29] A. A. Saharian, *Phys. Rev. D* **69**, 085005 (2004).